

AD-A248 163



1



AN EXAMINATION OF THE FEASIBILITY OF A NUCLEAR-
PUMPED LASER-DRIVEN INERTIAL CONFINEMENT FUSION
REACTOR WITH MAGNETICALLY PROTECTED WALLS

THESIS

John M. Jacobson, Captain, USAF

AFIT/GNE/ENP/92M-4

DTIC
ELECTE
APR 1 1992
S B D

92-08144



DISTRIBUTION STATEMENT A
Approved for public release;
Distribution Unlimited

DEPARTMENT OF THE AIR FORCE
AIR UNIVERSITY

AIR FORCE INSTITUTE OF TECHNOLOGY

Wright-Patterson Air Force Base, Ohio

92 8 31 093

REPORT DOCUMENTATION PAGE			Form Approved OMB No. 0704-0188	
Public reporting burden for this collection of information is estimated to average 1 hour per response, including the time for reviewing instructions, searching existing data sources, gathering and maintaining the data needed, and completing and reviewing the collection of information. Send comments regarding this burden estimate or any other aspect of this collection of information, including suggestions for reducing this burden, to Washington Headquarters Services, Directorate for Information Operations and Reports, 1215 Jefferson Davis Highway, Suite 1204, Arlington, VA 22202-4302, and to the Office of Management and Budget, Paperwork Reduction Project (0704-0188), Washington, DC 20503.				
1. AGENCY USE ONLY (Leave blank)	2. REPORT DATE March 1992	3. REPORT TYPE AND DATES COVERED Master's Thesis		
4. TITLE AND SUBTITLE AN EXAMINATION OF THE FEASIBILITY OF A NUCLEAR-PUMPED LASER-DRIVEN INERTIAL CONFINEMENT FUSION REACTOR WITH MAGNETICALLY PROTECTED WALLS		5. FUNDING NUMBERS		
6. AUTHOR(S) John M. Jacobson, Captain, USAF				
7. PERFORMING ORGANIZATION NAME(S) AND ADDRESS(ES) Air Force Institute of Technology, WPAFB OH, 45433-6583		8. PERFORMING ORGANIZATION REPORT NUMBER AFIT/GNE/ENP/92M-4		
9. SPONSORING / MONITORING AGENCY NAME(S) AND ADDRESS(ES)		10. SPONSORING / MONITORING AGENCY REPORT NUMBER		
11. SUPPLEMENTARY NOTES				
12a. DISTRIBUTION / AVAILABILITY STATEMENT Approved for public release; distribution unlimited		12b. DISTRIBUTION CODE		
13. ABSTRACT (Maximum 200 words) A preliminary design study of a nuclear-pumped laser-driven inertial confinement fusion reactor with a magnetically protected first wall using an advanced DT-ignited, DD-fueled pellet demonstrated the feasibility of such a concept. This paper presents a parametric study of the required energy multiplication in the blanket, the pellet injection rate, and the net efficiency of this conceptual reactor for advanced pellet yields. A model of the reactor energy balance yields a required energy multiplication of 2.4. A cylindrical design for a helium-cooled blanket demonstrates that natural uranium micropellets in a laser pump region provide a multiplication of 2.9 with a sub-critical neutron multiplication factor of 0.14. A lithium-oxide layer outside of the laser pump region provides a tritium breeding ratio of up to 0.4, which is more than sufficient to produce enough tritium for advanced DD-fueled, DT-ignited pellets to fuel the reactor. This paper presents the analysis behind these conclusions and presents avenues for further research on this concept.				
14. SUBJECT TERMS Nuclear-Pumped Laser, Inertial Confinement Fusion Reactor Tritium Breeding Ratio, Fission, Criticality		15. NUMBER OF PAGES 62		
		16. PRICE CODE		
17. SECURITY CLASSIFICATION OF REPORT Unclassified	18. SECURITY CLASSIFICATION OF THIS PAGE Unclassified	19. SECURITY CLASSIFICATION OF ABSTRACT Unclassified	20. LIMITATION OF ABSTRACT UL	

AFTT/GNE/ENP/92M-4

**AN EXAMINATION OF THE FEASIBILITY OF A NUCLEAR-
PUMPED LASER-DRIVEN INERTIAL CONFINEMENT FUSION
REACTOR WITH MAGNETICALLY PROTECTED WALLS**

THESIS

John M. Jacobson, Captain, USAF

AFTT/GNE/ENP/92M-4

Approved for public release; distribution unlimited

AN EXAMINATION OF THE FEASIBILITY OF A NUCLEAR-POWERED LASER-DRIVEN INERTIAL
CONFINEMENT FUSION REACTOR WITH MAGNETICALLY PROTECTED WALLS

THESIS

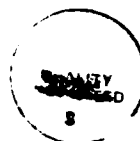
Presented to the Faculty of the School of Engineering
of the Air Force Institute of Technology
Air University
In Partial Fulfillment of the
Requirements for the Degree of
Master of Science in Nuclear Science

John M. Jacobson, B.S.
Captain, USAF

March 1992

Approved for public release; distribution unlimited

Accession For	
NTIS GRA&I	<input checked="checked" type="checkbox"/>
DTIC TAB	<input type="checkbox"/>
Unannounced	<input type="checkbox"/>
Justification	
By	
Distribution/	
Availability Codes	
Avail and/or	
Dist	Special
A-1	



Preface

I would like to thank Major Denis Beller at the Air Force Institute of Technology for his patience and guidance in acting as my thesis advisor during the performance of this study. I also thank Dr George Miley of the University of Illinois Fusion Studies Laboratory and Major Rick Hartley, Air Force Institute of Technology, for their suggestions during the project. Finally, I give my heart-felt thanks to my wife, Jennifer, and children, Amanda and Zach, for their support and consideration during my tenure at AFIT.

Table of Contents

Preface	ii
List of Figures	iv
List of Tables	vi
Abstract	vii
I. Introduction	1
Brief History	3
Overview	4
II. Description of Problem	5
Energy Flow Model	5
Blanket Neutronics	9
III. Results	14
Reactor Energy Balance	14
Effects of Varying ICF Pellet Yield Fractions	17
Effects of Blanket Geometry and Magnetic Diversion of Charged-Particles	20
Effects of Using DT-Fueled Pellets	23
Neutronics of Simple Reactor Blanket Model	24
Energy Multiplication in Simple Blanket Model	27
TBR for Simple Blanket Model	27
Effects of DT/DD Neutron Source Distribution on Neutronics.....	29
Helium-Cooled Blanket	30
Energy Multiplication and Criticality for He-Cooled Blanket	32
Tritium Breeding Ratio for He-Cooled Blanket	34
IV. Further Work	36
V. Summary	37
Appendix A: Energy Balance TK Solver Model	39
Appendix B: Sample MORSE Input File	42
Appendix C: Sample Mixing Input File	45
Appendix D: MORSE FORTRAN Code	46
Appendix E: Tritium Breeding Ratio TK Solver Model	52
Bibliography	54
Vita	55

List of Figures

Figure	Page
1. Energy flow diagram for a 1000-MWe plant	16
2. Required energy multiplication and pellet injection rate versus fusion neutron yield fraction	18
3. Reactor net efficiency versus fusion neutron yield fraction	19
4. Required energy multiplication and injection rate versus the x-ray yield fraction	20
5. Required energy multiplication, injection rate, and net efficiency versus aspect ratio	21
6. Injection rate and net efficiency versus fraction of charged-particle yield diverted to collectors	22
7. Required energy multiplication, injection rate, and net efficiency versus neutron yield fraction for a DT pellet	24
8. Geometrical model of the layers in a simplified design for the NPL-driven ICF reactor blanket initial neutronics calculations	26
9. TBR and average fusion neutron energy versus DT-ignitor yield fraction for a DD-fueled pellet	28
10. Cross-sectional view of the layers in a more detailed design for an He-cooled NPL-driven ICF reactor blanket neutronics calculations	31
11. TBR versus the volume of a He-cooled, natural Li ₂ O breeder	35

List of Tables

Table	Page
1. Average fission rate, TBR, and k versus percentage of DT source neutrons	30
2. Average fission rate, TBR, k, and calculated energy multiplication versus U-235 enrichment for helium-cooled blanket	32

Abstract

A preliminary design study of a Nuclear-Pumped-Laser-driven Inertial Confinement Fusion reactor with a magnetically protected first wall using an advanced DT-ignited, DD-fueled pellet demonstrated the feasibility of such a concept. A much smaller amount of electrical power is re-circulated than current ICF reactor designs with DT pellets because the O_2-I_2 laser is directly pumped by fissioning uranium micropellets in an O_2 gas with fusion neutrons. An overall reactor net efficiency of about 50% is achieved by converting fusion pellet energy into electrical energy because up to 75% of the pellet yield is in charged ions which can be converted directly into electrical current. The study indicated these factors could result in a reduced required driver yield of 5 MJ (vice 10 MJ currently projected) and a reduced pellet gain of 50 (vice 100 currently projected) for a feasible 1000-MWe power reactor operating with approximately 6 pellets per second. This paper presents a parametric study of the required energy multiplication in the blanket, the pellet injection rate, and the net efficiency of this conceptual reactor for advanced-pellet yield parameters. A model of the reactor energy balance yields a required energy multiplication of 2.4. A cylindrical design for a helium-cooled blanket demonstrates that natural uranium micropellets in a laser pump region provide an energy multiplication of 2.9 with a sub-critical multiplication factor of 0.14. A self-sustaining plant which produces enough tritium for advanced DT-ignited, DD-fueled ICF pellets requires a tritium breeding ratio of 0.4 or less, depending on the yield fraction of the DT ignitor. A natural lithium-oxide breeder with a volume of 140 m^3 surrounding the fission pump region produced a TBR of 0.42. The volume can be reduced substantially if the DT-ignitor yield fraction is 0.15 or less. These considerations define avenues for further research for this reactor concept.

AN EXAMINATION OF THE FEASIBILITY OF A NUCLEAR-PUMPED LASER-DRIVEN INERTIAL CONFINEMENT FUSION REACTOR WITH MAGNETICALLY PROTECTED WALLS

I. Introduction

Inertial confinement fusion (ICF) reactors in which the energy released from the implosion and subsequent fusion of deuterium-tritium (DT) pellets is converted to electrical energy are under intense study because they promise greater safety than current fission reactors and may be more economic than fission or fossil-fuel energy plants. They are inherently more safe than current fission reactors because any failure in the system stops the fusion process, whereas the fission process may continue after a mechanical failure. ICF reactors are also attractive because there are no highly radioactive fission products to store after the fuel is burned, only neutron-activated materials whose radioactivity decays away much more quickly than fission products. These radioactive wastes can generally be treated as low-level or medium-level wastes (shielding may be required) that are easier to dispose than the high-level wastes (shielding and cooling required) generated in fission plants. ICF reactors may be more economic than fission or fossil-fuel reactors if the tritium required to produce the fuel pellets can be furnished by the reactor itself. If this is the case, the major expense of an ICF reactor is the capital for building the plant, after which the only operating expenses will be for deuterium, which is extractable from water, and plant maintenance. This means, for example, that US dependence on overseas oil or foreign uranium supplies for its energy production would be greatly reduced. Thus, safety and economy could make an ICF reactor very attractive.

One current design of a future commercial ICF reactor envisions using a large laser (10 MJ per pulse) to implode high-gain DT-fueled pellets (1000 MJ per pellet) at a few pellets per second with the fusion energy captured in a blanket surrounding the pellet and converted to electrical energy through a thermal cycle such as a gas turbine (1:14-15). In order to store the energy required to power the laser between pulses, huge banks of capacitors are required and a significant amount of the electrical energy generated must be recycled to feed the laser. A second drawback of such a design is that most of the energy released by a DT-fueled pellet is in neutrons (up to 80%). These neutrons are used to produce electricity through a thermal conversion process such as steam or a gas

turbine which has a potential efficiency of 30-45%. In contrast, the charged-particle yield of the fusion event has the potential to produce electricity through direct conversion at an efficiency of 60-90% (2:38). An obvious way to improve the design of a commercial ICF reactor is to develop a more efficient laser which is directly driven by the fusion event itself and thus decrease the amount of recycled electrical energy. In addition, the efficiency can be improved by using an advanced-fuel pellet which has a greater charged-particle yield fraction so that direct conversion may be used. The higher reactor net efficiency resulting from these improvements would reduce the required pellet gain.

A design that holds promise for a more efficient laser driver for an ICF reactor is the nuclear-pumped laser (NPL). With this design, the population inversion in the laser pump medium is directly driven by fissions induced in either a coating surrounding the pump gas or in micropellets in an aerosol. There have been a number of gaseous media investigated for possible use in a nuclear-pumped laser, including lasers pumped with uranium-coated and boron-coated tubes as well as lasers pumped with the ionizing material (UF_6 , ^3He , and uranium-bearing micropellets) mixed with the gas. Representative examples include Ne- N_2 , Xe- F_2 , CO, He-Xe, XeO, KrF, Ar-Xe, and many others (3:1367). Uranium-bearing micropellets have been found to be the most efficient means for exciting a pumping gas. In this design, fusion neutrons from the ICF pellet cause fissions in uranium-containing microspheres of order of 1-10 μm in radius. The fission fragments escape from the micropellet with an efficiency up to 80% for a UO_2 microsphere (4:208) and decelerate in the pump gas by ionization and excitation of the gas molecules. High-energy secondary electrons produced in this process continue the process of ionization and excitation until a secondary electron gas with an average electron energy of about 15 eV is produced. An attractive pump medium under these conditions is O_2 , which has a favorable excitation cross-section for its first excited state ($^1\Delta$) at this electron energy (5:15). Another favorable aspect is that at pumping pressures of 0.1 atm with a buffer gas (such as argon) to limit O_2 de-excitation through collisions of several atmospheres, the residence time of the $\text{O}_2(^1\Delta)$ state is several milliseconds (4:17). This might allow one to store energy in the excited oxygen to permit laser firings on the order of 10 per second or less, the projected rate for a commercial ICF laser driver. $\text{O}_2(^1\Delta)$ has a near resonance with the excited state ($^2\text{P}_{1/2}$) of iodine which emits at 1.31 μm and could be used to drive a fusion pellet implosion (5:15). Thus, the $\text{O}_2\text{-I}_2$ nuclear-pumped laser could be attractive as an efficient future ICF driver.

A second improvement in the design efficiency of a commercial ICF reactor is to capitalize on the high efficiency with which charged-particle energy can be converted to electrical energy by increasing the fraction of the fusion pellet yield in charged particles. Advanced-fuel pellets with deuterium-deuterium (DD) or deuterium-helium 3 (D^3He) fuel, ignited by a small DT ignitor in the center, offer the possibility of greatly enhancing the charged-particle fraction of the yield compared to that of DT-fueled pellets. The yield from a fusion pellet is partitioned into x rays, neutrons, and charged particles. For a normal DT-fueled pellet, up to 80% of the energy is carried away by neutrons. For advanced-fuel pellets, however, the charged-particle yield fraction can be as high as 75%, with much smaller neutron yield fractions (6:703). If the neutron energy is sufficient to drive the NPL, this type of pellet could be used to greatly increase the net efficiency of an ICF reactor provided the charged particles emitted by the fusion event are channeled to collector plates for direct conversion.

Brief History

To take advantage of the increased efficiencies associated with a nuclear-pumped laser and converting charged-particle yield into electricity, Beller and others proposed a NPL-driven ICF commercial reactor design fueled by advanced D^3He -fueled pellets (7:772). The conceptual reactor they studied consisted of a spherical blanket with a 5-m-radius cavity surrounding the imploded pellets. The x-ray or thermal fraction of the yield was absorbed in the first wall of the blanket and converted to electrical energy through a thermal process with an efficiency of 40%. A magnetic field directed the charged particles from the fusion event to collector plates for direct conversion to electricity at an assumed efficiency of 85%. Finally, the neutron fraction of the pellet yield entered a fissioning region in the blanket containing enriched uranium and oxygen where the neutrons produced fissions to power an O_2-I_2 laser. Surrounding the fission blanket was a lithium-containing blanket to produce tritium for replenishing that used in the DT ignitor. A graphite reflector formed the outermost region of the blanket. A fraction of the fission energy produced pumped the laser for the next shot (40%), while the remaining low-grade fission and neutron energy was converted to electricity through a thermal process at 33% efficiency.

The initial study by Beller and others demonstrated the feasibility of the concept of an NPL-driven ICF reactor (7:777). D^3He -fueled pellets with yields of 250 MJ could be inserted into the reactor cavity at approximately 6 pellets per second to power a 1000 MWe plant at a net efficiency of 53%. Furthermore, the fission energy required to power a 5-MJ laser was provided by uranium

enrichments of 1-10% in a 100-cm thick fission blanket behind the graphite first wall. Thus, a fusion pellet gain of 50 was conceptually acceptable. This gain is half that which is currently projected to be required for a feasible DT-pellet reactor, making the requirements for technological advances for a commercial ICF reactor more manageable. A tritium-breeding ratio (TBR) of greater than 1 (per source neutron) was possible with various sized Li-containing regions meaning a more than adequate supply of tritium could be produced. The study thus suggested that the concept of an NPL-driven ICF is attractive should an NPL and advanced-fuel pellets become available.

Overview

This paper presents a further analysis of the energy balance and neutronics associated with the design of an O₂-I₂ NPL-driven commercial ICF reactor with a magnetically protected first wall. A model of the plant energy balance provides a basis for a simple parametric study of the factors involved in designing the reactor. A 1000-MWe plant fueled by advanced-fuel pellets (DD or D³He as the major fuel) appears feasible with 250-MJ pellets at approximately six pellets per second with an assumed O₂-I₂ laser net efficiency of 8% and a required energy multiplication in the blanket of 2.4. An examination of the effects of DT-fueled versus advanced-fuel pellets on the design and net efficiency of the reactor indicate the desirability of developing an advanced-fuel pellet for this type of reactor.

The neutronics of the plant, namely, the number of fissions per source neutron and TBR are examined using a cylindrical blanket, because this is a natural configuration for flowing a pump gas and coolant along the longitudinal magnetic lines necessary to direct the charged particles to collector plates (2:244). Calculations performed using the MORSE Monte Carlo transport code demonstrate that a blanket of reasonable size containing natural uranium or low-enriched uranium micropellets in the laser pump aerosol could yield an energy multiplication of 2.9 (20% more than required) or more with a sub-critical multiplication factor of 0.14 and negligible fuel burn-up over periods of a year or greater. If future studies require more fission energy, the effect of changing the uranium enrichment on the fission rate (hence neutron energy multiplication) and blanket criticality is provided. Likewise, the tritium breeding ratio required for self-sustained operation with advanced DD-fueled pellets is 0.4 or less (for a DT-ignitor yield fraction of 50% or less). The TBR calculated for a Li₂O breeder of 140 m³ was 0.42, so self-sustained operation is feasible. Finally, the blanket neutronics indicate there is a wide range of coolants, pump gas constituents and partial pressures, and material compositions possible which do not affect the fission rate appreciably.

II. Description of Problem

Two design aspects of a NPL-driven commercial ICF reactor with magnetically protected walls have been modeled: the energy flow for a 1000-MWe plant and the neutronics of a cylindrical blanket. The energy flow, represented by a system of simultaneous equations, has been modeled using a TK-Solver routine. The routine allows the user to vary parameters such as the neutron yield fraction and observe the effects on the overall plant energy balance. The MORSE Monte Carlo transport program provided the means for calculating the number of fissions per source neutron and TBR for a cylindrical reactor blanket. Then, for an assumed number of source neutrons based on the ICF pellet yield, one can calculate the energy multiplication in the blanket as well as determine if the reactor produces enough tritium for sustained operations.

Energy Flow Model

A TK Solver routine consisting of a set of simultaneous equations provided a model for examining the energy flow in a NPL-driven ICF reactor with magnetically protected walls and an O₂-I₂ laser. The model consisted of a characterization of the yield of an advanced-fuel pellet and a set of efficiencies for converting that yield into electrical energy and a laser pulse for imploding the next fuel pellet. The average powers produced by the various conversion processes were calculated by multiplying the energy available from that process per pellet by the pellet injection rate.

The first part in the process of creating energy is the fusion event itself. This requires that an ICF pellet be imploded by the laser driver with some driver energy, W_d . This in turn will drive the production of fusion energy by creating a burn wave in the pellet, producing a fusion yield from the pellet, W_f . The gain of the pellet, Q , can then be defined as the fusion yield of the pellet over the laser driver energy $Q = W_f / W_d$. Typically, the yield from an ICF pellet is partitioned into an x-ray fraction, f_x , a neutron fraction, f_n , and a charged-particle or plasma fraction, f_c . One requires that

$$f_x + f_n + f_c = 1$$

so that the three forms of energy considered for conversion to electricity are x rays or radiation, neutrons, and charged particles such as alpha particles, deuterons, tritons, etc. The yields associated with these three forms are thus $W_x = f_x W_f$ where W_x is the x-ray yield, $W_n = f_n W_f$ where W_n is the neutron yield, and $W_c = f_c W_f$ where W_c is the charged-particle yield. Because the charged-particle yield can theoretically be converted to electricity at efficiencies approaching 90%,

the greater the amount of ions which can be diverted from the blanket first wall to collectors at the ends of the cylindrically shaped blanket, the more efficient the whole plant will be. This process is hindered slightly by the conversion of some of the charged-particle yield into radiation via recombination, bremsstrahlung, and cyclotron radiation and by charged particles which are not diverted to the collector plates by the external magnetic field (9:328). The kinetic energy of these particles must be absorbed by the first wall and converted to electrical energy by a thermal process. Thus, the fraction of charged-particle yield converted into radiation, f_{rad} , and the efficiency with which charged particles are diverted by the magnetic field to the collector plates for direct conversion, f_B , both affect the amount of energy available for direct conversion, W_{dc} , where

$$W_{dc} = f_B (1 - f_{rad}) W_c$$

The energy available for direct conversion produces electrical energy with an efficiency, η_{dc} , such that $W_{dc,e} = \eta_{dc} W_{dc}$ where $W_{dc,e}$ is the electrical energy produced by direct conversion. The direct conversion energy loss is then $W_{dc,l} = W_{dc} - W_{dc,e}$.

Another process producing electricity in the plant is the conversion of the radiation and charged-particle yield which is absorbed in the blanket and first wall by a thermal cycle. The radiation energy available in the reactor cavity is the x-ray yield plus the charged-particle yield converted into radiation, i. e., $W_{rad} = (W_x + f_{rad} W_c)$ where W_{rad} is the radiation energy available for thermal conversion after absorption in the first wall. A cylindrical blanket differs from a spherical blanket in that part of the radiation and neutron yields could be lost if the ends of the blanket are not fully enclosed. Also, the fact that not all of the neutrons from the fusion event will make it into the cylindrical fissioning region of the blanket limits the fraction of the neutron yield available for driving the population inversion of the laser. To take these factors into consideration, the reactor performance was degraded slightly by incorporating a blanket geometry factor, f_g , which reduced the amount of neutron and radiation yield absorbed in the first wall. The geometry factor was set equal to the fractional solid angle subtended at the center of the reactor cavity by the ends of the cylinder

$$f_g = 1 - \frac{1}{\sqrt{4AR^2 + 1}}$$

where f_g is the geometry factor and AR , the aspect ratio, is the cylinder radius in m divided by the cylinder length in m. The radiation and charged-particle energy reaching the cylindrical first wall are converted to electricity with a thermal efficiency, η_{th} , so that the total electrical energy produced by thermal conversion in the first wall is

$$W_{fw,e} = (1 - f_g) \eta_{th} (W_{rad} + (1 - f_B)(1 - f_{rad}) W_c)$$

where $W_{fw,e}$ is the electrical energy produced by thermal conversion of the energy absorbed in the first wall and η_{th} is the thermal conversion efficiency for this process (a gas turbine, for example). The thermal energy lost in the blanket can be written

$$W_{fw,l} = (1 - \eta_{th}) \frac{W_{fw,e}}{\eta_{th}}$$

where $W_{fw,l}$ is the thermal energy lost in the first wall.

The neutron fraction of the fusion yield is multiplied in the fission blanket and converted into energy to pump the O₂-I₂ laser and into electricity via a low-grade thermal conversion process. A fraction of the fusion neutrons entering the uranium and oxygen mixture causes fissions with approximately 200 MeV of energy released per fission (32 MeV in neutrons and 168 MeV in fission fragments). The fission fragments are then available to excite O₂ molecules in the aerosol. The required energy multiplication, M , of the neutron yield in the fission blanket is defined as $M = W_{fiss} / W_n$ where W_{fiss} is the total fission energy released in the blanket. The efficiency with which fission-fragment energy is converted into excitation energy in the oxygen gas is dependent on two processes: the efficiency with which the fission fragments escape from the uranium-bearing micropellets, η_{ff} , and the efficiency with which escaped fragments excite the singlet-delta state of oxygen molecules in the gas, η_{ex} . Therefore, the energy stored in excited O₂ molecules in the cylindrical fission region is

$$W_{n,ex} = (1 - f_g) M W_n (168/200) \eta_{ff} \eta_{ex}$$

where $W_{n,ex}$ is the excitation energy of the oxygen gas and only a portion of the neutron yield is available to cause fissions in the blanket because of the geometry factor degradation. The fraction of fusion neutrons which do not cause fissions, the fraction of radiation not absorbed in the first wall,

the fission energy which is not used to excite O₂ molecules, and the waste heat from the laser are present as lower-grade thermal energy available for conversion to electricity by a thermal process. This thermal energy is

$$W_{n,th} = W_n (1 + M(1 - \eta_{ff} \eta_{ex} (168/200))) + W_{d,l} + f_g W_{rad}$$

where $W_{d,l}$ is the lower-grade thermal energy produced by the iodine laser. Part of this lower-grade thermal energy can be converted to electrical energy so that

$$W_{n,th,e} = \eta_{lg} W_{n,th}$$

where $W_{n,th,e}$ is the electric energy produced from the lower-grade thermal energy detailed above and η_{lg} is the efficiency with which thermal energy in the blanket and laser is converted to electricity. The low-grade thermal energy loss is then $W_{n,th,l} = W_{n,th} - W_{n,th,e}$.

The excitation energy stored in the oxygen gas, $W_{n,ex}$, is used to pump an iodine laser by flowing the oxygen gas into a cavity containing I₂. There are two efficiencies associated with forming and targeting the laser pulse. The excited O₂ molecules must first give up their energy to iodine molecules to excite the iodine gas. Then, the laser optics shape and deliver the pulse on target. The two efficiencies associated with these processes are the chemical exchange efficiency between the oxygen and iodine, η_{ch} , and the optical efficiency of creating, shaping, and targeting a laser pulse, η_{opt} . Thus, the final driver energy delivered to the target by the laser is

$$W_d = \eta_{ch} \eta_{opt} W_{n,ex}$$

where W_d is the laser driver energy put on target. The energy loss in producing a laser pulse is simply $W_{d,l} = W_{n,ex} - W_d$.

The net results of the energy flow model of the NPL-driven ICF reactor are that there is a total energy per pellet available for conversion to electricity

$$W_{tot} = W_c + W_x + W_{n,th}$$

and total electrical energy produced per pellet

$$W_{elec} = W_{fw,e} + W_{dc,e} + W_{n,th,e}$$

The net efficiency, η_{net} , of the plant is then $\eta_{net} = (W_{elec} - W_{rec}) / W_{tot}$ where W_{rec} is the electrical energy re-circulated to operate the plant (pumps, control systems, etc.) which is assumed to be 150 MWe for a 1000-MWe NPL-driven ICF reactor.

This summary has presented the major relations used in the energy balance model for an NPL-driven ICF reactor with magnetically protected walls. The reader is referred to Appendix A for more details of the TK model used.

Blanket Neutronics

The neutron economy of a NPL-driven ICF was studied using the MORSE Monte Carlo transport program which is capable of handling detailed three-dimensional geometries. The MORSE code is essentially a collection of subroutines which can be modified or called by the user as desired to calculate neutron fluxes or fluences, reaction rates, etc. for a specific geometry containing specified media (9). A multiple-batch mode was selected in which 10 batches of fusion source neutrons were used to calculate the mean and fractional standard deviation of the fission rate, tritium-breeding reactions per source neutron or TBR, and average neutron multiplication factor, k . For a fissioning system, this is defined as the neutrons produced in the current generation divided by the neutrons in the last generation. A critical blanket would have a k of 1, while a k less than one indicates the blanket is subcritical. The basic components of the MORSE model developed to examine the blanket neutronics were a fusion neutron source, a simplified geometry representing the regions composing a cylindrical blanket, and a main FORTRAN program which calculated the fissions per source neutron, TBR, and k . The content of each of these components follows.

The source of neutrons from each fusion event, specified in a MORSE input file (see Appendix B), contained the source location (in Cartesian coordinates) and the energy distribution of the fusion neutrons emitted. The source was modeled as an isotropic point source located at the center of the reactor cavity. The DABL69 46-neutron, 23-photon group library developed by Oak Ridge National Laboratory provided the broad-group energy-dependent cross sections used with the transport code (8:7-11). Thus, the source energy spectrum for an advanced DT-ignited, DD-fueled pellet had DT reaction neutrons at 14.1 MeV in energy group 4 (13.8-14.2 MeV) and DDn reaction neutrons at 2.45 MeV in group 17 (2.4-3.0 MeV). The initial assumption was that 87% of the source neutrons were DT neutrons and 13% were DDn neutrons based on a previous study of a DT-ignited, DD-fueled pellet (6:703).

The MORSE geometry model of a cylindrical blanket consisted of a series of connected right circular cylinders and truncated cones. Zones containing the blanket first wall, coolant chambers, fissioning region, Li-bearing region for tritium breeding, and a reflector/plenum were specified by logically adding or subtracting the cylinders and cones. Each zone was a homogeneous mixture of the materials or isotopes present in that zone (see Appendix C for an example of a cross-section mixing file which specifies how the microscopic cross sections are mixed to produce the macroscopic cross sections for each homogeneous MORSE zone). The inner diameter of the first wall was chosen to be 5 m to prevent sublimation of a graphite wall for a 250-MJ pellet with up to 25% of its energy released as x rays (7:776). A length of 15 m for the cylindrical portion of the blanket was chosen to increase the volume intersected by neutrons released from the fusion event while still maintaining a reasonably sized reactor. To increase the number of neutrons reflected back into the cylindrical portion and the amount of x-ray energy absorbed, the ends of the blanket first wall and its coolant region were modeled as truncated cones which necked down to an opening of 0.5-m in diameter. As a result, the overall blanket length measured 19 m.

The results of a MORSE Monte Carlo run were determined by a user-written FORTRAN routine which specified how MORSE calculates the neutron fluence in the fissioning region, the fissions per source neutron, and the TBR in any Li-bearing layers (see Appendix D). In general, the contribution to the total neutron fluence by a source neutron in a zone is

$$F = \frac{TRK}{VOL}$$

where F is the fluence in neutron-cm/cm³, TRK is the weighted path length traveled by a neutron in the zone volume in cm, and VOL is the volume of the zone in cm³. A weighted path length is used because MORSE employs survival biasing. This means that a particle is not killed by a collision resulting in absorption. Rather, the particle weight at each collision is reduced by the ratio of Σ_s / Σ_t , where Σ_s is the macroscopic scattering cross-section and Σ_t is the macroscopic total cross-section. The statistics of the Monte Carlo estimates are improved by increasing the number of particles which contribute to the average of any quantity, so that particles with reduced weights are used until they are killed by Russian Roulette when their weight drops below some preset value.

The weighted path length, TRK , is computed differently for zone boundary crossings and collisions. At a boundary crossing,

$$TRK = WATE \sqrt{(x - x_0)^2 + (y - y_0)^2 + (z - z_0)^2}$$

where $WATE$ equals the current weight of the neutron, the coordinates (x, y, z) represent the location of the neutron at the boundary crossing, and the coordinates (x_0, y_0, z_0) represent the location of the neutron's last interaction. At a collision, on the other hand,

$$TRK = WTBC \sqrt{(x - x_0)^2 + (y - y_0)^2 + (z - z_0)^2}$$

where $WTBC$ is the weight of the neutron before a collision, and (x, y, z) represent the location of the collision. Since path length estimators are used to calculate the fission rate and TBR, the true weight of the neutron while it traveled the given path must be used.

Once the fluence or path length is known, the number of fissions which occur in the fissioning zone can easily be calculated. The number of fissions occurring in the pump gas zone per source neutron is simply

$$N_f = (F)(VOL)(\Sigma_f)$$

where N_f is the total number of fissions occurring in the volume per source neutron, and Σ_f is the macroscopic fission cross section in cm^{-1} . MORSE does not provide Σ_f as a variable, but does provide $PNUF$ which is defined for an energy group as

$$PNUF = \frac{\nu \Sigma_f}{\Sigma_t}$$

where ν is the average number of fission neutrons emitted for a specific energy group and Σ_t is the total macroscopic cross section for the group in cm^{-1} (9:4.5-23). Thus, recalling that fluence per source neutron is the path length per particle divided by the volume and substituting for Σ_f after solving the equation above, the equation for N_f is simply

$$N_f = \frac{(TRK)(PNUF)(\Sigma_t)}{\nu}$$

The numerator is calculated in the main MORSE routine. The division by ν is accomplished by multiplying the result for each energy group by $\frac{1}{\nu}$ for that group (specified in a response matrix in the input file). The final value for N_f is computed by summing over all interactions and all energy

groups. To get the total number of fissions in a batch (or total fission weight if source and fission particles initially have a weight of one), N_f is multiplied by the number of source particles in that batch.

To get an average, MORSE then sums the results for all source neutrons in a batch, divides by the number of source neutrons per batch, and calculates the average number of fissions per source neutron and the fractional standard deviation by using the results from the number of batches specified by the user. The results depend somewhat on the number of batches chosen, but for this study, 10 batches appeared to provide adequate statistics.

The number of tritium-breeding reactions per source neutron (TBR) was calculated in a similar fashion. Tritium is bred in ^6Li when a neutron is absorbed and undergoes the reaction $^6\text{Li}(n,\alpha)\text{T}$, the cross section for which increases from 0.02 barn at the high-energy end of the spectrum to 753 barn for thermal neutrons. Tritium can also be bred in ^7Li by the reaction $^7\text{Li}(n,n',\alpha)\text{T}$. However, this reaction is endothermic and can only occur for neutron energies greater than 2.47 MeV. Its cross section is less than 0.04 barn even at the high-end of the energy spectrum. The macroscopic cross section for breeding tritium in the Li-bearing zones of the blanket was calculated in the main FORTRAN code by inputting the number densities of ^6Li and ^7Li in the region (in atoms/barn-cm) and multiplying by the microscopic cross sections (in barns) for each of the above reactions to derive the macroscopic cross sections for tritium-breeding reactions for each of the 46 energy groups. The total tritium-breeding cross section for each group was then the sum of the two. (As the Li-reaction group cross sections for the DABL69 46-group library were unavailable, cross sections were interpolated from the DLC-31 37-neutron-group library (7:7-11).) An argument similar to that provided above for calculating fissions yields the following for the number of tritium-breeding reactions occurring in a Li-bearing zone:

$$N_T = (TRK)(\Sigma_{TBR})$$

where N_T is the total amount of tritium bred in the volume, and Σ_{TBR} is the macroscopic tritium-breeding cross section for Li. The results are tabulated by MORSE on a per source neutron basis for each batch and the average and fractional standard deviation were calculated for 10 batches of neutrons.

In addition to the fission and tritium breeding ratio, the criticality of the blanket fission region was of interest because a subcritical blanket is safer and does not require neutronic control. The criticality of the blanket can be calculated in two ways. One method is to use the number of fission neutrons produced per batch and divide by the number of source neutrons to calculate k . An average k is then computed by summing the results of all the batches and dividing by the number of batches. The other method is to simulate generations of fission neutrons. With this method, the source of neutrons for the next batch is the collection of fission neutrons from the previous batch. The criticality is then computed by taking the number of neutrons in each batch and dividing by the number in the previous batch. In both cases, where k was less than 0.2, the fissions died out in four generations after the initial fusion event, and the criticality calculated was the same to two significant digits. Thus, the criticality was primarily calculated by dividing the total weight at the end of a batch of the fission neutrons generated in that batch by the initial weight of the batch source particles. An average k and its standard deviation were then calculated by running 10 batches and allowing MORSE to calculate the statistics for the results.

The parameters of interest, fissions per source neutron, TBR, and criticality, were calculated in the manner outlined above. The primary focus of the study was to identify the feasibility of and trends for an NPL-driven ICF reactor with a cylindrical blanket. To this end, the number of source neutrons was varied from 1000 to 5000 per batch to keep the fractional standard deviations for the average values calculated in the 1-3% range.

III. Results

The results of the study of a conceptual O₂-I₂ NPL-driven ICF commercial reactor with magnetically protected walls are dependent upon pellet yield fractions and assumed plant efficiencies which affect the overall energy balance of the plant and the neutron economy of potential blanket designs. The results from the energy balance study suggest that if the published efficiencies for this type of laser and the various means of energy conversion can be realized, the NPL-driven ICF reactor could have a net efficiency somewhere near 50%, making it a very attractive concept. Likewise, if advanced-fuel ICF pellets with neutron and charged-particle yields near those assumed become available, the reactor may be able to operate with natural uranium or even depleted uranium micropellets in the fissioning layer. It could also function as a net tritium breeder (if this is politically expedient), because even a small amount of lithium oxide in a breeding layer produces more than enough tritium to sustain the plant (assuming the DT ignitor yield for the advanced-fuel pellets is less than about 10% of the total pellet yield).

Reactor Energy Balance

The energy balance or power cycle for the plant is detailed in Figure 1. The O₂-I₂ NPL is driven by fusion-neutron induced fissions in the blanket with a total laser efficiency of

$$\eta_l = \eta_{ff} \eta_{ex} \eta_{ch} \eta_{opt} = 0.08$$

where $\eta_{ff} = 0.8$ is the fission fragment escape efficiency, $\eta_{ex} = 0.5$ is the efficiency with which fission fragments excite the oxygen molecules in the pumping mixture, $\eta_{ch} = 0.5$ is the efficiency for converting the excitation energy carried by oxygen molecules into excitation energy in a population inversion in the iodine, and $\eta_{opt} = 0.4$ is the efficiency of converting that population inversion into a laser pulse on the pellet (6:772-773). The laser is directly powered by fusion neutrons entering the pump mixture which contains uranium-bearing micropellets and oxygen gas. Argon gas is also present to act as a buffer to reduce collisions between excited O₂ molecules or excited O₂ molecules and the reactor first wall, thus minimizing the loss of excitation energy by collisional processes. The amount of excitation energy carried into an iodine pumping region by excited O₂ molecules is dependent on the energy multiplication which occurs in the fission blanket. This required energy multiplication, M , is defined as the total fission energy produced in the blanket per pellet divided by the total fusion neutron yield of the pellet W_{fiss}/W_n . Thus, M represents the energy multiplication

required to allow the plant to produce 1000 MWe and to power the laser. For a reactor fueled with 250-MJ pellets with an x-ray yield of 25 MJ, a neutron yield of 38 MJ, and a charged-particle yield of 187 MJ, the required energy multiplication is 2.4 (for a cylindrical blanket 10 m in diameter and 15 m in length).

In addition to powering the laser to implode another advanced-fuel pellet and thus continue the process of producing energy, the yield from the pellet must also be converted into electricity as efficiently as possible. In the plant model developed, electricity production occurs through a thermal cycle converting the radiation and part of the charged-particle energy produced by the fusion event (10%) absorbed by the blanket first wall at an assumed efficiency of 40%. A very small percentage of the charged-particle yield is converted into radiation by processes such as bremsstrahlung, recombination, line radiation, and cyclotron radiation. This fraction is smaller than 1% of the charged-particle yield, however, for magnetic fields on the order of 1T and electron temperatures of about 10 keV (11:62-70) with ion and electron number densities of 10^{20} per cm^3 (typically assumed conditions for an ICF plasma). Most of the electricity is produced by converting the charged-particle yield of the pellet diverted to collector plates at the ends of the blanket (90% assumed) into electricity. The conversion process changes the kinetic energy of the ions into potential energy by applying a stopping voltage across the plates. This direct conversion has an assumed efficiency of 85% for the ions and electrons which reach the plates. Finally, the neutron and fission fragment energy which does not contribute to the excitation energy carried by the O_2 gas, a small fraction of the radiation and charged-particle energy which is not absorbed in the first wall, and the waste heat from the iodine laser produce low-grade heat in the reactor which must be removed by coolant and which could supplement electricity production through a thermal process. The efficiency for converting this low-grade thermal energy in the blanket and laser into electricity is assumed to be 33%.

With the efficiencies and the pellet parameters outlined above, the model of the reactor energy balance can be used to calculate the number of pellets per second required to produce 1000 MWe. A 1000-MWe plant with 150 MWe recirculated to run pumps and power the control system and other auxiliary systems requires a pellet injection rate, R_{inj} , of about six pellets per second, which is within currently projected capabilities of 1-10 pellets per second for future ICF reactors. The net efficiency for the plant is 51%. Thus, with a required energy multiplication of 2.4, this reactor is potentially a very efficient fusion power plant.

Effects of Varying ICF Pellet Yield Fractions. The exact characteristics of future advanced-fuel pellets are currently unknown. Initial calculations indicate the x-ray and neutron yield fractions for advanced-fuel pellets may vary from less than 10% to around 30%, while charged-particle yield fractions may vary from 60-75% (6:703). An examination of the effects on the baseline design for the plant caused by varying the neutron yield fraction (hence, varying the charged-particle yield fraction) at a constant x-ray yield fraction of 10% for pellet gains of 25 (125 MJ fusion output), 50 (250 MJ fusion output), and 100 (500 MJ fusion output) is shown in Figure 2. The plot indicates that higher-gain pellets require less energy multiplication in the fission blanket and fewer pellets per second to operate since more fusion energy per laser pulse is produced. For a pellet of specified gain, the required energy multiplication decreases rapidly as the fusion neutron fraction increases from about 5 to 15% and less rapidly from about 15% to 35%. This is due to the increase in the neutron yield which, for a constant required fission yield determined by the laser pulse requirement of 5 MJ and the laser efficiency, decreases M . The injection rate, however, increases linearly with the fusion neutron yield fraction since the conversion-efficient charged-particle yield fraction is decreasing and more pellets per second are required to produce 1000 MWe.

The variation in net plant efficiency with the fusion neutron yield fraction at a constant x-ray fraction of 10% for the same pellet gains appears in Figure 3. The net efficiency of the plant increases with increasing pellet gain since more fusion energy per laser pulse is produced and thus more energy is available for conversion to electricity per pulse. For an advanced-fuel pellet with a particular gain, the reactor net efficiency decreases linearly with increasing neutron yield fraction because more fusion energy per pellet is in neutrons vice charged-particles. Thus, less energy per pellet is converted to electricity by the high-efficiency direct conversion process, reducing the net efficiency of the plant. For a 250-MJ pellet ($Q = 50$), the net efficiency drops from about 54% to 45% as the neutron yield fraction increases from 5% to 35%. Figures 1 and 2 indicate that the smallest neutron yield fraction consistent with a realizable energy multiplication in the blanket is desirable.

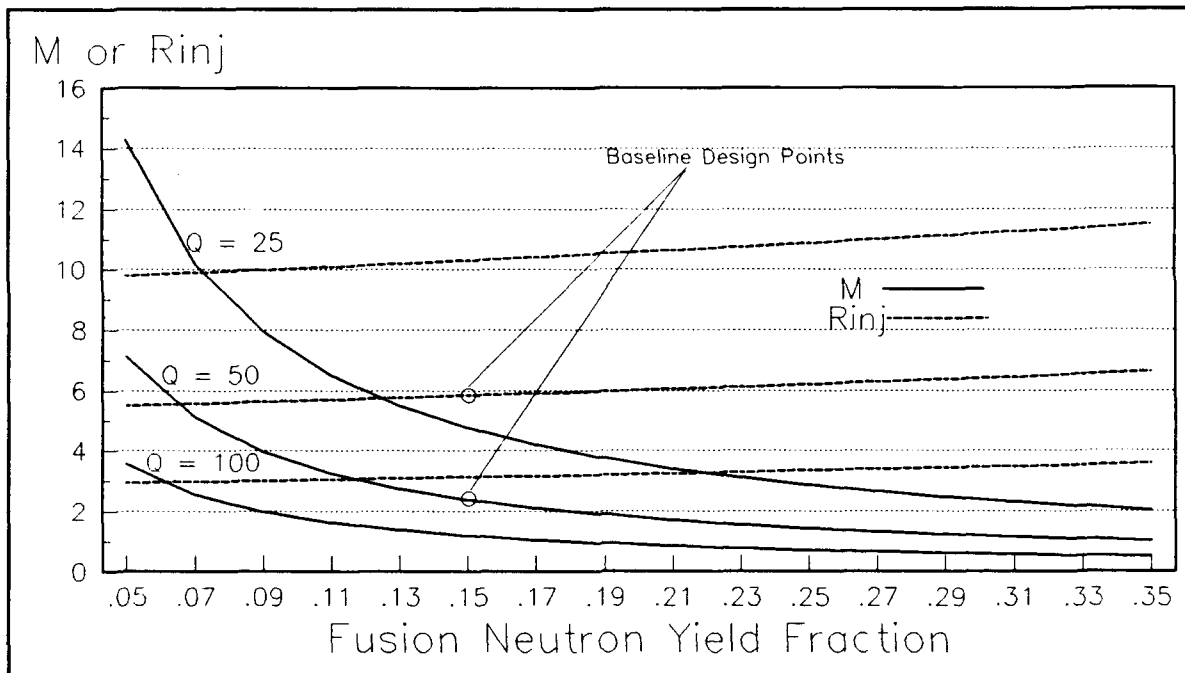


Figure 2. Required energy multiplication, M , and injection rate, R_{inj} , versus fusion neutron yield fraction, f_n .

(Other parameters as in Figure 1 with $f_x = 0.10$.)

The variation of the pellet injection rate, R_{inj} , and the required energy multiplication, M , with the x-ray yield fraction of an advanced-fuel ICF pellet is provided in Figure 4 for a 250-MJ pellet with a constant charged-particle yield fraction of 60%. The pellet injection rate does not depend significantly on the x-ray yield fraction because the bulk of the electricity is produced by direct conversion of the charged-particle yield. Likewise, the net efficiency of the plant does not vary by more than 1% over the x-ray fractions indicated, decreasing from 47% to 46%. However, as the x-ray yield fraction increases from 5% to 33%, and thus the neutron yield fraction decreases from 35% to 7%, M increases by a factor of five since there is a reduced number of neutrons which must still produce the same amount of total fission energy to power the laser. Thus, reducing the amount of x-ray yield in relation to the neutron yield of the ICF pellet will reduce the energy production requirement for the fission blanket without significantly altering the plant performance.

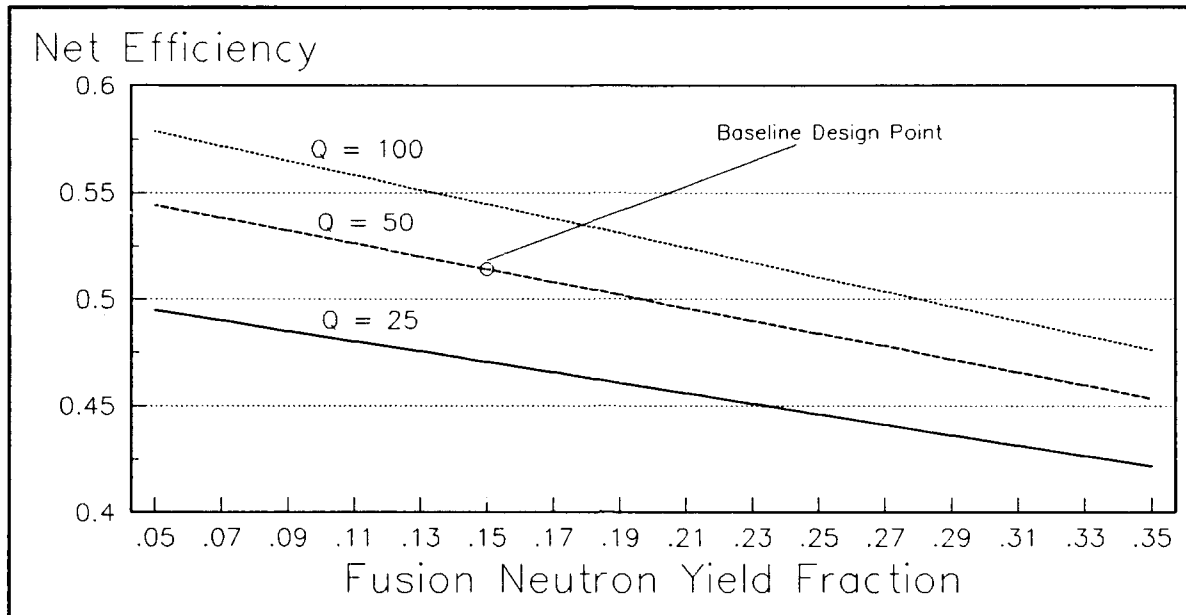


Figure 3. Reactor net efficiency, η_{net} , versus fusion neutron yield fraction, f_n .
(Other parameters as in Figure 1 with $f_x = 0.10$.)

The effects of varying the x-ray, neutron, and charged-particle yield fractions of a 250-MJ pellet have been outline above. The figures indicate that there is a large parameter space in which the plant can operate with reasonable energy multiplications, injection rates, and high net efficiencies. However, as the x-ray yield fraction approaches 30%, or as the fusion neutron fraction decreases to a few percent, the required energy multiplication increases to 5 or 6. This is probably too high. On the other hand, as the charged-particle yield fraction decreases to below 50%, the injection rate increases to about 7 Hz and the net plant efficiency decreases to about 45%, which are still reasonable values. Thus, the energy balance model indicates that the plant is robust to changes in these parameters, but a pellet with fractions near $f_x = 0.10$, $f_c = 0.75$, and $f_n = 0.15$ as in the baseline design is desirable.

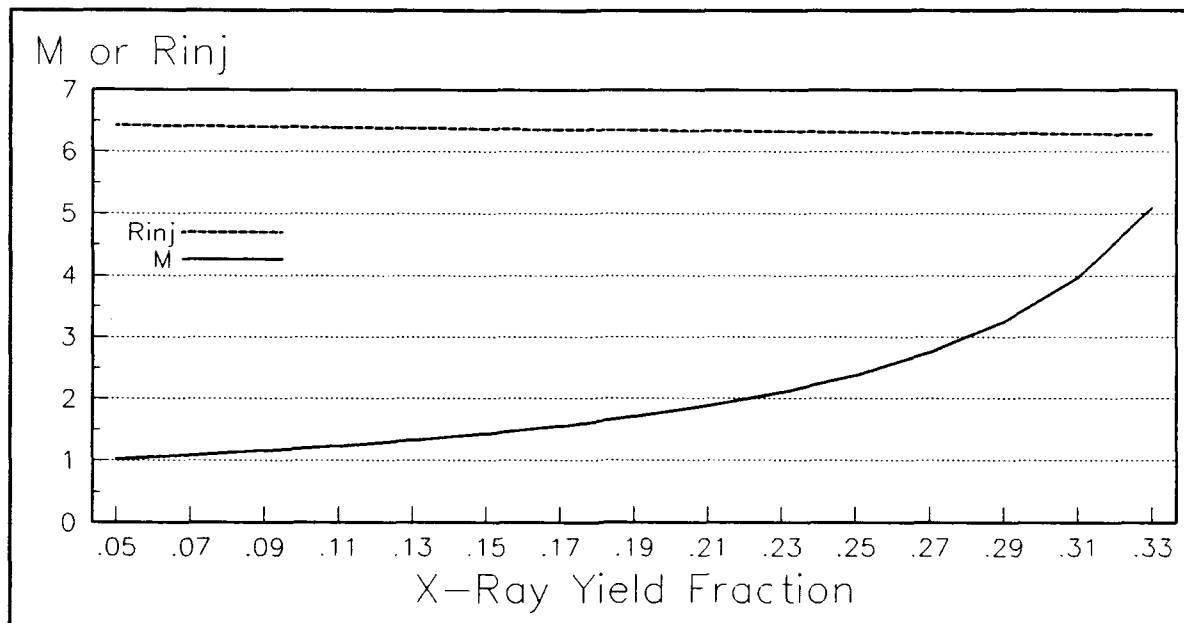


Figure 4. Required energy multiplication, M , and injection rate, R_{inj} , versus the x-ray yield fraction, f_x .

(Other parameters as in Figure 1 with $f_c = 0.60$.)

Effects of Blanket Geometry and Magnetic Diversion of Charged Particles. The energy balance model used to examine the plant power cycle included a geometry factor simulating the degradation of the energy multiplication in the blanket fission layer because of less than 100% total coverage of the fusion neutron source. The amount of radiation absorbed by the first wall was also reduced by the geometry factor so that some of the energy which would have been converted to electricity after impinging on the first wall went into the low-grade heat produced in the blanket instead, thus producing electricity by a less efficient process. Even with a spherical blanket, some of the energy released by the pellet would not be absorbed by the first wall since up to 10% of the first wall area would be required for openings for the laser beams. Thus, the geometry factor, which is simply the fractional solid angle subtended by the ends of the cylinder at the center of the cavity, was an attempt to model a cylindrically shaped blanket and obtain a conservative estimate of the required energy multiplication for the reactor.

For a cylindrical blanket with a 5-m radius and a 15-m length as assumed in Figure 1 (aspect ratio of 0.33), the geometry factor is 0.17. Because the geometry factor depends on the aspect ratio (R/L) of the blanket, an examination of the effect of varying the aspect ratio on the required energy multiplication, the pellet injection rate, and the net efficiency was undertaken. Figure 5 shows M increases with increasing aspect ratio (decreasing fission blanket coverage) while η_{net} decreases. The pellet injection rate, R_{inj} , is not significantly changed, however, because the direct collection of charged particles diverted by the external magnetic field - the primary determinant of R_{inj} - was held constant. The figure indicates that blanket aspect ratios higher than about 0.33 are undesirable unless a significant amount of neutrons can be reflected back into the fission region. There is a trade-off, however, between increasing the coverage of the reactor cavity provided by the first wall (by adding truncated conical sections, for example) and making the opening at the ends of the blanket large enough for a charged-particle energy flux which will not melt the direct conversion collector plates. Thus, both of these factors must be taken into account in determining the geometry of the blanket for this reactor.

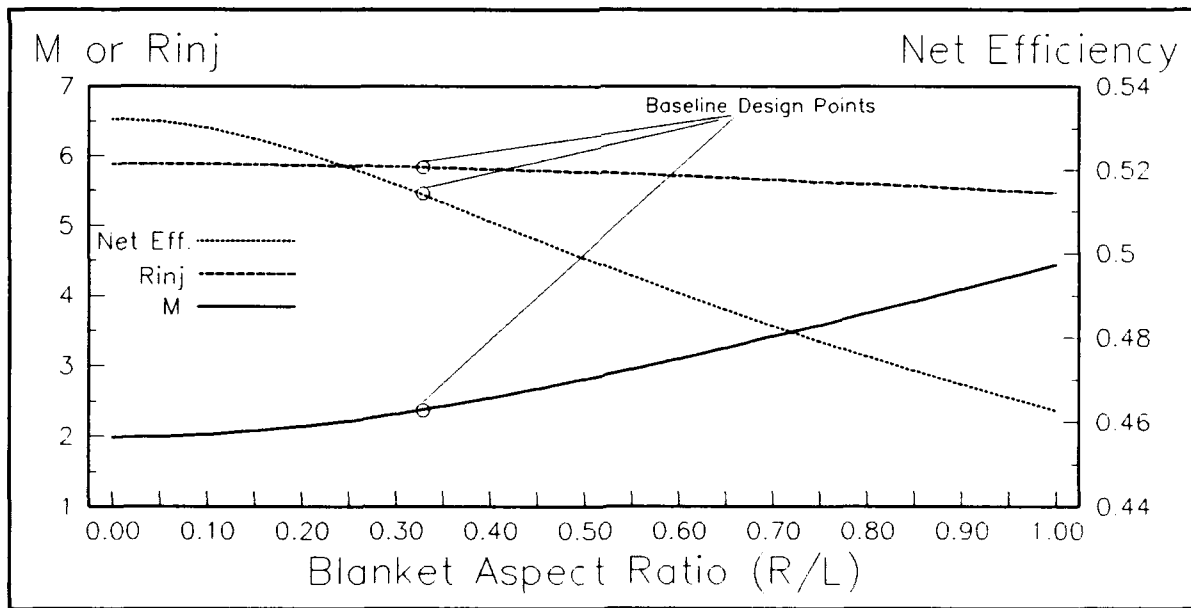


Figure 5. Required energy multiplication, M , injection rate, R_{inj} , and net efficiency, η_{net} , versus aspect ratio.
(Other parameters as in Figure 1.)

The two important parameters affecting the required pellet injection rate for pellets of a particular gain are the fraction of fusion yield available as charged particles or ions and the efficiency with which these particles are diverted by the magnetic field to collector plates at the ends of the blanket for direct conversion to electricity. The effect of the second factor on the pellet injection rate and the reactor net efficiency is seen in Figure 6. Calculating the actual trajectories of charged particles emitted by an ICF pellet is difficult and requires assumptions about the location and distribution of simulated fusion particles before the magneto-hydrodynamic equations can be used to move particles for a particular set of coils (12:391-394). In lieu of a detailed calculation, the study simply varied the fraction, f_B , of ions and electrons reaching the collector plates from 50% to 90%. As Figure 6 indicates, the pellet injection rate required to maintain 1000 MWe decreases from about 7.2 to 5.8 over this interval, while the net efficiency increases from 41% to 51%. Clearly, one would like to collect as much of the charged-particle yield as possible for direct conversion, but even if only 50% of the charged-particle yield of a 250-MJ pellet is collected, the plant is still 41% efficient and the number of pellets per second increases by only one to two, still within the bounds considered technologically feasible.

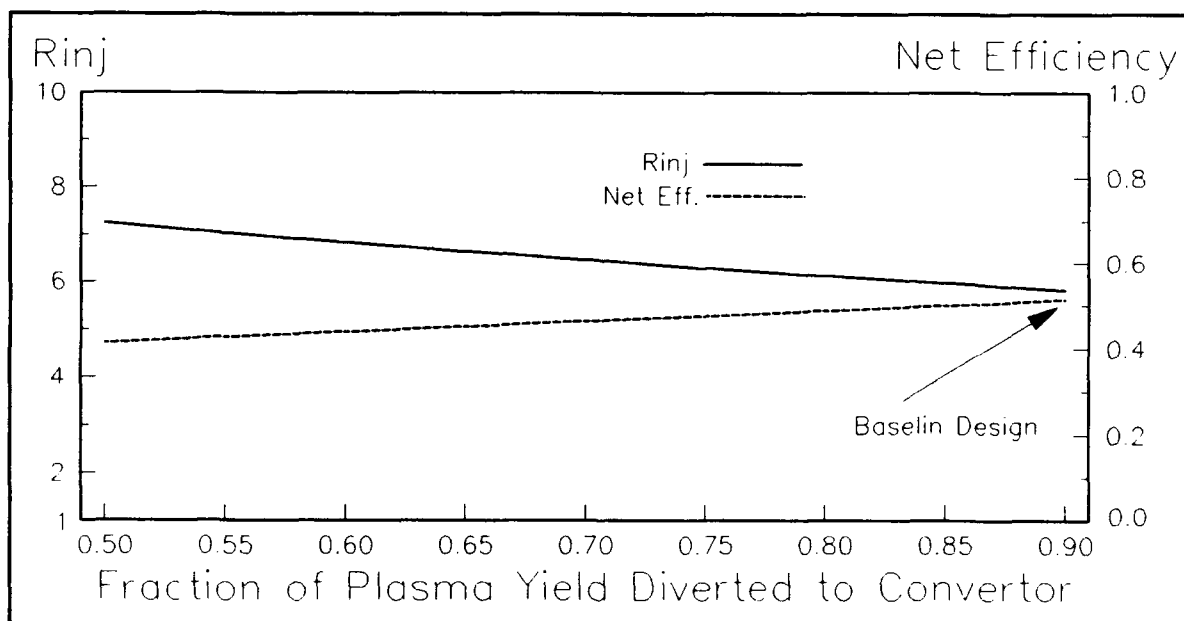


Figure 6. Injection Rate, R_{inj} , and net efficiency, η_{net} , versus fraction of charged-particle yield, W_c , diverted to collectors.
(Other parameters as in Figure 1.)

The effects of changing the geometry factor or aspect ratio and the fraction of charged particles diverted to the collectors have been examined. The parameter study of the geometry factor suggest that an aspect ratio for the reactor cavity greater than about 0.33 induces a degradation in reactor performance by doubling the required energy multiplication and decreasing the net efficiency by 6-7%. As the diverted-particle fraction decreases from the baseline design of 0.9 to 0.5, the injection rate increases by about 1 pellet per second, but the net efficiency of the plant drops by about 10%. Thus, a low aspect ratio and a high diversion of charged particles to the collectors are important aspects of this conceptual NPL-driven ICF reactor.

Effects of Using DT-Fueled Pellets. The power cycle resulting from the energy balance model demonstrates that a 1000-MWe reactor with a net efficiency near 50% and realistic pellet injection rates may be possible for the O₂-I₂ NPL-driven ICF reactor if advanced-fuel pellets with the characteristics assumed become available. If DT-ignited DD- or D³He-fueled pellets cannot be realized in the future, however, the effect of relying on DT-fueled pellets to fuel the reactor is presented in Figure 7. The theoretical neutron yield fraction of a DT pellet is 80%. However, actual pellet fractions will probably be somewhat less as some of the fusion neutrons released do not escape from the pellets. Figure 7 shows that for 250-MJ DT pellets ignited by 5-MJ laser pulses, the required energy multiplication is 20% of that associated with advanced fuel pellets and decreases slightly with increasing neutron yield as before. The net plant efficiency is also smaller (between 33% and 38%) because the percentage of energy available as charged particles is substantially reduced. Finally, the pellet injection rate increases by 2-3 pellets per second to account for the decreased reactor efficiency.

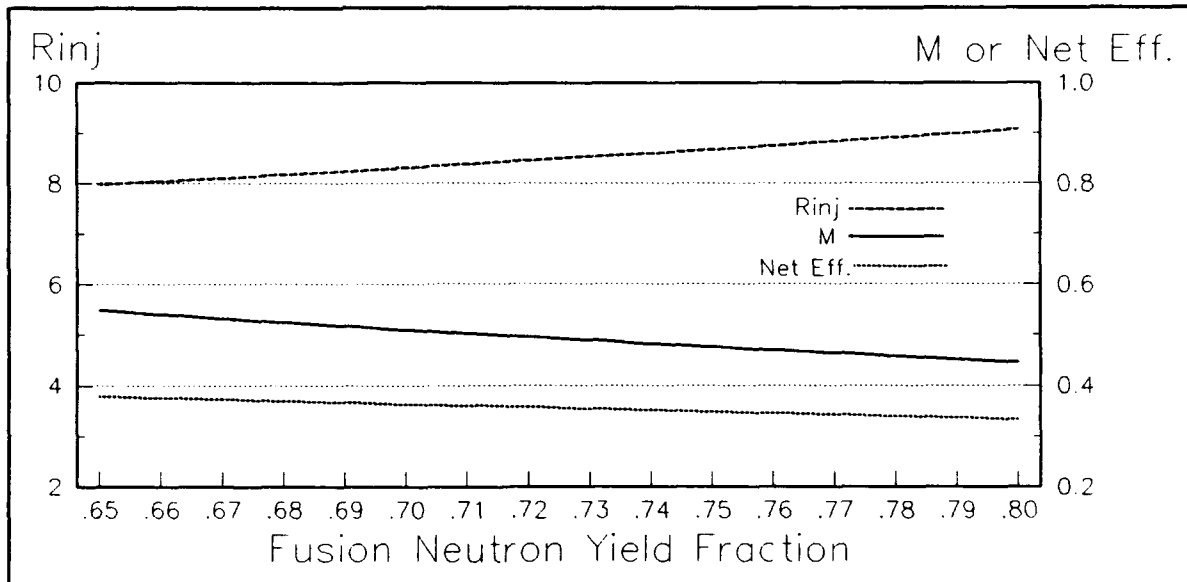


Figure 7. Required energy multiplication, M , injection rate, R_{inj} , and net efficiency, η_{net} , versus neutron yield fraction, f_n , for a DT pellet.
(Other parameters as in Figure 1 with $f_x = 0.05$.)

Neutronics of Simple Reactor Blanket Model

The energy balance model developed for the NPL-driven ICF reactor with a magnetically protected first wall required an energy multiplication of 2.4 in the fissioning region of the blanket for the plant to operate with the baseline parameter values in Figure 1. To examine the feasibility of obtaining an energy multiplication of this magnitude, as well as the feasibility of producing enough tritium in one or more lithium-containing layers to sustain the operation of a reactor fueled by advanced-fuel DD pellets, the MORSE Monte Carlo transport code was utilized with a cylindrically shaped blanket as shown in Figure 8.

This simple blanket model used to examine the trade-offs of a cylindrically shaped blanket consisted of a cavity at vacuum with a fusion neutron isotropic point source at the center surrounded by a first wall with a cylindrical section 10 m in diameter and 15 m in length. To improve neutron reflection into the fission layer (and radiation absorption in an actual reactor), the ends of the first wall cylinder were capped with truncated conical segments 2 m in length which necked down to 0.5 m in diameter. This opening would be required for collecting the fusion charged-particle yield for direct

conversion, with some type of neutron trap to capture neutrons escaping from the cavity (2:78). The first wall was assumed to be graphite and was 8 cm thick (over 40 mean free paths thick for 10 keV x-rays). Outside the first wall ran a coolant layer/tritium-breeder 4 cm thick. A 68-cm-thick fissioning region containing uranium, oxygen, and argon surrounded the blanket first wall and coolant layer. This homogeneous region represented the NPL pump gas mixture containing oxygen and uranium oxide micropellets which would flow axially along the blanket (along the magnetic field lines) before being directed out of the blanket where the oxygen could then be mixed with iodine to produce a 1.31- μ m pulse. Outside the fissioning region was a cylindrical coolant/tritium-breeding layer 8 cm thick and an 8-cm-thick graphite reflector and shield.

The results of a series of MORSE runs calculating the blanket energy multiplication and TBR with this model are presented in the following sub-sections. An analysis of the importance of the DT/DD neutron source distribution is also included.

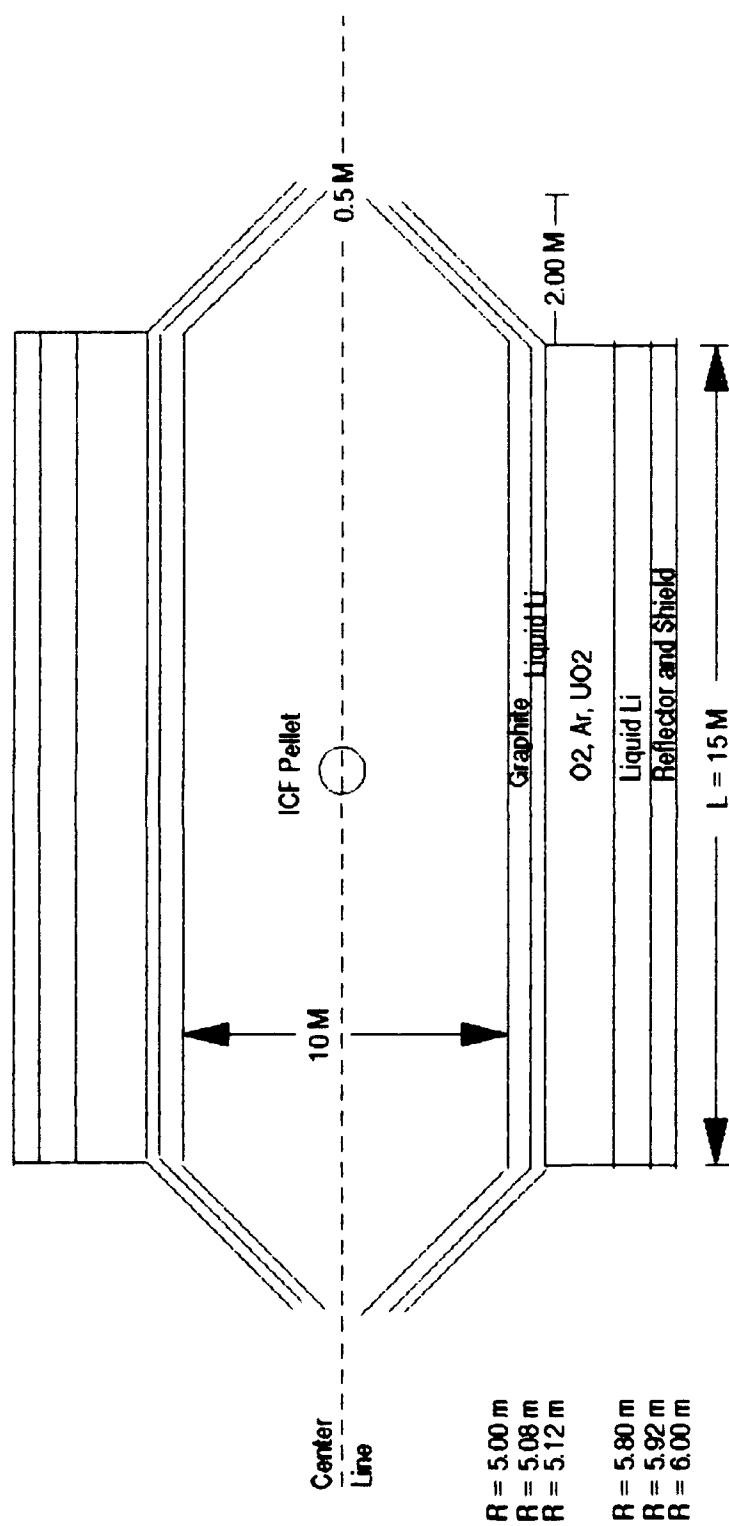


Figure 8. Cross-sectional view of the layers in a simplified design for the NPL-driven ICF reactor blanket initial neutronics calculations.

Energy Multiplication in Simple Blanket Model. The first blanket examined contained liquid lithium in the coolant layers, serving as both a coolant and tritium-breeder. The homogeneous fissioning region modelled represented UO_2 1-micrometer micropellets with natural uranium at a density of 4.9×10^{15} micropellets/ m^3 (a 98% void) and O_2 gas at 1 atm. For this configuration, the number of fissions per source neutron was 0.026. Most fissions occur at the high-energy end of the spectrum (1-14 MeV) as the 8-cm-thick first wall does not really moderate fusion neutrons. Also, ^{238}U (99.3% of natural uranium) has a fission cross-section which decreases with energy. (As higher enrichments of ^{235}U are required, the thickness of the first wall can be increased to reduce the fusion neutron energy to the epithermal and thermal part of the spectrum where the fission cross section for ^{235}U is much greater. In fact, for highly enriched uranium (40% or higher), the optimum first wall thickness appeared to be 16-24 cm.) Assuming a 250-MJ pellet with 15% ($W_n = 37.5$ MJ) neutron yield, 43.6×10^{16} neutrons/MJ released (6:703), and 200 MeV (3.204×10^{-17} MJ) per fission, this equates to an energy multiplication (W_{fiss} / W_n) of 2.4. This was sufficient to satisfy the required energy multiplication obtained from the energy balance model. The blanket average neutron multiplication, k , was 0.13, so the blanket was very subcritical. However, this analysis for the energy multiplication is very dependent the number of escape neutrons assumed.

The effects of changing the pump gas conditions and micropellet make-up were examined by modelling the fission layer with oxygen at 0.1 atm, argon at 1 atm, and UC_2 micropellets (which might reduce unwanted recombination of excited O_2 molecules to the micropellets). The fission rate per source neutron and the blanket criticality remained unchanged. Thus, the energy multiplication in the pump gas mixture and the blanket criticality are essentially independent of the gaseous constituents and their partial pressures, providing latitude in the choice of constituents for the nuclear-pumped region of an NPL. The energy multiplication and fission blanket criticality is dependent on the total amount of uranium and the enrichment included in the fissioning layer, allowing the designer to increase the volume, density, or enrichment of the uranium-containing layer if greater energy multiplication is required.

TBR for Simple Blanket Model. The tritium-breeding capabilities of this blanket model were examined. The results are presented below as the number of T-breeding reactions in lithium per source neutron, the blanket TBR. This presentation of the results differs slightly from that normally seen in fusion blanket studies for DT-fueled fusion pellets where the TBR is always greater than one.

This is because every triton which fuses in a DT reaction produces one 14.1-MeV neutron. In order to conserve the plant tritium inventory for a self-sustaining operation, therefore, for every fusion neutron produced there must be at least one triton produced. In actuality, the required blanket TBR must be greater than one to account for the fact that not all fusion neutrons make it to the blanket, the decay of tritium (half-life of 12 yr), and the fact that the tritium collection process will be something less than 100% efficient. With an advanced DD-fueled pellet containing a DT-ignitor, however, the TBR for self-sustaining operation can be much less than one because each fusion event has only to produce enough tritium to supply an ignitor for another pellet. The TBR required for D^3He -fueled pellets is similarly less than one.

Figure 9 depicts the variation in the TBR required to sustain plant operation and the average source neutron energy as a function of the fraction of a DD-fueled pellet fusion yield produced by a DT-ignitor (see Appendix E for details). The results show that the required TBR is 0.1 or less for DT-ignitor fractions of 15% and 0.4 for ignitor yield fractions of 50%. Thus, the required TBR for the plant with advanced pellets will ultimately depend on the size of the DT-ignitor required to start a burn wave in a DD-fueled pellet.

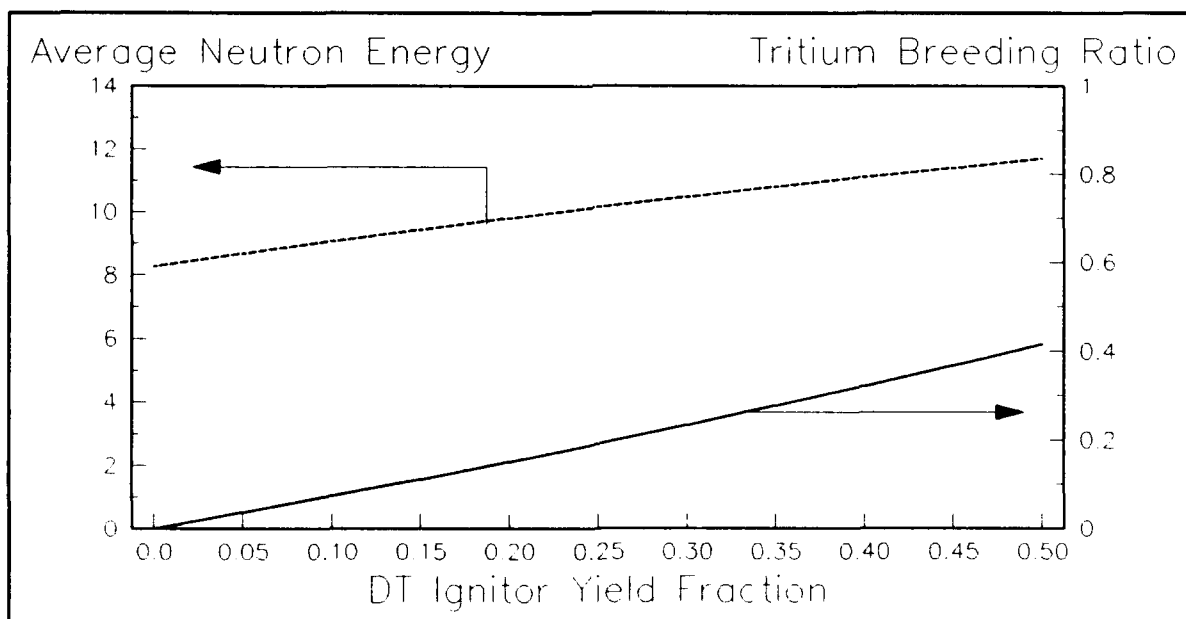


Figure 9. TBR and average fusion neutron energy versus DT-ignitor yield fraction for a DD-fueled pellet.

Liquid lithium has been considered as a possible coolant for ICF reactors because it can also serve as a tritium breeder and thus satisfy two functions at once. Natural lithium contains atom abundances of 7.5% ^6Li and 92.5% ^7Li , both of which undergo reactions which produce tritium. The ^6Li reaction of interest is the $^6\text{Li}(n,^4\text{He})\text{T}$ reaction which has a cross section which increases from about 0.03 barn for 14-MeV neutrons to over 750 barn for thermal neutrons. Tritium is produced in ^7Li by the reaction $^7\text{Li}(n,n',^4\text{He})\text{T}$ which is an endothermic reaction and requires neutrons with energies higher than 2.47 MeV to occur, meaning DDn neutrons (2.45 MeV) cannot react with ^7Li to produce tritium. The cross section for this reaction is less than 0.04 barn for all energies between 2.5 and 14.1 MeV. As a result, tritium production from ^7Li is generally negligible (1-2 orders of magnitude smaller) when compared to that produced by ^6Li , even for lithium which is not enriched in ^6Li .

A blanket design with natural liquid-lithium in both coolant layers yielded a TBR of over 0.1. This would be sufficient (when compared to the required TBR in Figure 9) to sustain an NPL-driven ICF reactor with advanced DD-fueled pellets having ignitor yields less than 15%. By enriching the ^6Li in the liquid-lithium first layer to 80% abundance, the TBR increased to over 0.4, which is the TBR required for an ignitor yield of 50% (essentially, a hybrid DT/DD ICF pellet). Thus, a blanket with 120 m^3 of liquid lithium in the configuration of Figure 8 would produce more than enough tritium for a reactor operated with advanced-fuel DD pellets, and could actually serve as a net tritium breeder, if this is required at some future date.

Effects of DT/DD Neutron Source Distribution on Neutronics. Because the results of this study are the product of an assumption of the percentage of DT (14.1 MeV) versus DDn (2.45 MeV) source neutrons (see Chapter II), which will only be confirmed by future experiment, a quick study of the effects of varying the relative percentages of DT and DDn source neutrons on the fission rate and TBR was performed. Table 1 shows the results of varying the energy distribution of source neutrons from 50% DT and 50% DDn neutrons to 100% DT neutrons for the blanket in Figure 8. The results indicate that the blanket TBR is not very sensitive to the ICF source energy distribution, while the fission rate varies by approximately 50%. This variation is large, but does not change the energy multiplication in the blanket by an order of magnitude. A more important factor in determining the multiplication is the number of escape neutrons from the ICF pellet. Calculations show this varies by an order of magnitude or more depending on the final density of the ICF pellet and ignitor after implosion, and on whether a DD-fueled or D^3He -fueled pellet is considered (6:703).

TABLE 1 AVERAGE FISSION RATE, TBR, AND k VERSUS PERCENTAGE OF DT SOURCE NEUTRONS			
PERCENT DT SOURCE NEU- TRONS (DT/(DT + DDn))	FISSIONS PER SOURCE NEUTRON	TBR	AVERAGE k FOR FUSION NEUTRONS
50	0.0206 + /-1%	0.111 + /-5%	0.0919 + /-.0022
87	0.0266 + /-1%	0.111 + /-4%	0.1288 + /-.0018
100	0.0290 + /-1%	0.101 + /-6%	0.1412 + /-.0024

Helium-Cooled Blanket

The initial blanket design indicated that the fission rate necessary to produce the required energy multiplication and the TBR required to sustain an operational advanced-fuel reactor could be feasibly obtained with a reasonably sized, subcritical blanket and relatively small Li-containing regions. To discover if these results continued to hold for a more detailed design, a proposed helium-cooled blanket with realistic amounts of HT-9 steel was modelled (13).

Figure 10 presents a cross-sectional view of the blanket geometrical model used with the MORSE transport code. The homogeneous-zone model consisted of a cavity filled with air at 0.01 atm, a first wall 10 cm thick, a 360-m³ fissioning region composed of UC₂ micropellets at 4.9 x 10¹⁵ per cubic meter (UC₂ at 98% void), O₂ at 0.1 atm, argon at 1 atm, and 10% glass (representing flow tubes for the laser pump aerosol), a 285-m³ breeder containing Li₂O, a 25-cm thick plenum for neutron reflection and energy absorption, and a 30-cm thick shield composed of iron, chromium, and nickel. Realistic amounts of HT-9 steel for an actual blanket were included in each homogeneous layer, and the open spaces in the blanket were filled with a mixture of air, copper (for magnet coils) and glass.

The following sub-sections present the energy multiplication, criticality, and TBR for this He-cooled blanket. An analysis of the effects of changing the gas pressures in the fission region is included in the sub-section on energy multiplication. An estimate of fuel burn-up for a reactor of this type is also presented in this sub-section.

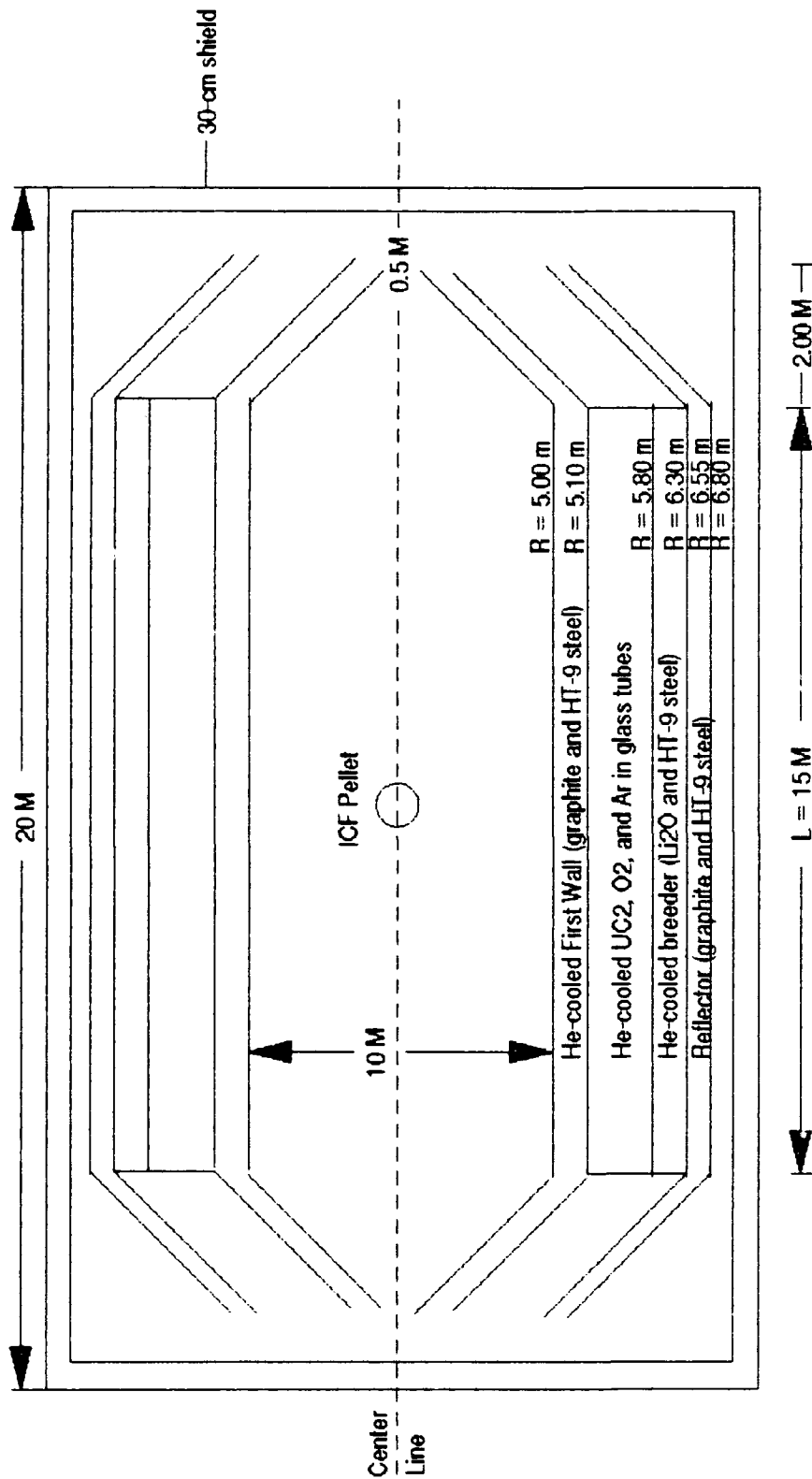


Figure 10. Cross-sectional view of layers in a more detailed design for a He-cooled NPL-driven ICF reactor blanket neutronics calculations.

Energy Multiplication and Criticality for He-cooled Blanket. Table 2 provides the fission rate per source neutron, TBR, average criticality, and calculated energy multiplication for various ^{235}U enrichments in the fission region of the He-cooled blanket portrayed in Figure 10. The energy multiplication calculated is strongly dependent on the number of escape neutrons which must be assumed. The study indicated that the blanket criticality at 40% enrichment was approximately 0.8. This value is probably approaching the upper limit desirable for the blanket. However, the energy multiplication calculated for the blanket indicates that the reactor may very well operate with natural uranium micropellets (calculated M of 2.9 is higher than the 2.4 required by the energy balance for the base-line design), in which case the blanket is very far from critical, and will remain so with a loss of pressure in the fissioning pump region. Thus, determining the number of pellet escape neutrons used in the calculation of the energy multiplication will be important in determining the enrichment and criticality for any future blanket design.

TABLE 2				
AVERAGE FISSION RATE, TBR, k, AND CALCULATED ENERGY MULTIPLICATION VERSUS U-235 ENRICHMENT FOR HELIUM-COOLED BLANKET				
U-235 ENRICHMENT	FISSION RATE*	T-BREEDING REACTIONS*	AVERAGE k	CALCULATED M**
0.72% (NAT)	0.032	0.46	0.140 +/-0.001	2.9
10%	0.086	0.50	0.286 +/-0.002	8.0
20%	0.14	0.55	0.441 +/-0.003	14
40%	0.28	0.62	0.800 +/-0.001	26
* Average fission rate and T-breeding reactions per neutron values have Monte Carlo fractional standard deviations of less than 1%.				
** Calculated assuming 43.6×10^{16} escape neutrons per MJ, 250-MJ pellet, and 200 MeV per fission. Neutron yield as in Figure 1.				

The results in Table 2 also indicate that the fission rate per source neutron for the detailed model are slightly higher (0.032 vice 0.026) than that obtained with the simplified model since more neutrons are reflected into the fissioning region. However, the fission rate is not significantly dependent on the amount of glass or copper present or the pressure or type of coolant, unless highly enriched liquid lithium is used. In fact, because helium is not as corrosive as lithium is, and because a small amount of lithium is required for tritium breeding in the blanket, it is probably the coolant of

choice for an advanced-fuel ICF reactor. The neutronics of the blanket do not depend significantly on the helium pressure, and are not affected by realistic levels of steel and copper in the blanket, so the fission rate and criticality calculations are robust for a wide range of blanket designs.

In addition to the feasibility of obtaining a required blanket energy multiplication, the reactor designer is also interested in the fuel burn-up for an operating reactor since this will determine how often new fuel must be purchased and how fast poisons and radioactive fission products build up in the fission layer. For natural uranium with a fission rate per source neutron of 0.032, 1.09×10^{20} neutrons per 250-MJ pellet, and an injection rate of six pellets per second, the burn-up of uranium is 0.4% per year, assuming no flow in the fission layer. In actuality, the burn-up will be less than this value, so the reactor can operate for extended periods of time before fuel replacement is necessary.

Another concern for the designer of an O_2-I_2 NPL-driven ICF reactor is whether there are enough O_2 molecules in the fissioning region to store the excitation energy for pumping the iodine. With a 360-m^3 pumping region for the He-cooled blanket in Figure 10, the number of O_2 molecules available for excitation at a partial pressure of 0.1 atm is 10^{28} . A partial pressure of 0.1 atm for oxygen is expected to result in an energy storage time of hundreds of milliseconds (4:17) which is the order of magnitude required to produce laser pulses at a frequency of 1-10 per second. To support the 25 MJ of energy required to pump the assumed 5-MJ iodine laser, 4×10^{26} excited molecules are required (the $^1\Delta$ state of O_2 carries 0.98 eV of energy). This yields an excited-to-ground-state ratio of 0.04 which is less than the minimum ratio of 0.17 that initial studies indicate is required to effectively pump iodine with oxygen in a chemical laser (4:15). However, as the fission rate and energy multiplication are not dependent on the pressure of the oxygen gas in the pumping region, the partial O_2 pressure can be reduced to 0.01 atm. This increases the ratio to 0.4 without affecting the neutronics significantly. The independence of the neutronics on the partial pressures of the oxygen and a buffer gas like argon provides the designer with leeway to optimize the aerosol mixture for laser pumping efficiency. Alternatively, one could reduce the volume of the fissioning region and increase the enrichment of the uranium to get a higher excited-to-ground-state ratio at a pressure of 0.1 atm and the same energy multiplication.

In summary, the NPL-driven ICF reactor can attain a energy multiplication of 2.9 which is higher than the required energy multiplication of 2.4 with natural uranium in the fission region, for a variety of different partial pressures for the laser pump gas and with low burn-up. The criticality of

the blanket under this condition is 0.14, and a loss-of-pressure accident which caused the uranium micropellets to pool would not result in a critical geometry. However, these results are strongly dependent on the assumption of the number of source neutrons escaping from the fusion event.

Tritium Breeding Ratio for He-cooled Blanket. The second part of the neutron economy equation is the TBR of the He-cooled blanket. The variation of the blanket TBR with breeder volume for a breeder containing natural Li_2O located outside of the fissioning region is shown in Figure 11. Even with a 5-cm-thick breeder (volume of 27 m^3), a TBR of greater than 0.2 resulted. When compared to the required TBR in Figure 9, this TBR is sufficient to support DD-fueled pellets with up to 25% of their yield provided by a DT ignitor. In fact, a tritium breeder may not be required with an advanced-fuel pellet. Initial calculations have indicated that a sufficient amount of tritium may be bred in DD- or D^3He -fueled ICF pellets for continuous reactor operations (6:702-703). Thus, the TBR obtainable with a He-cooled Li_2O breeder is greater than the TBR required for an ICF reactor operating with advanced-fuel pellets for the volumes indicated on Figure 11. This indicates that a very small breeder (only a few cubic meters) is required for the NPL-driven ICF reactor baseline design if the DT-ignitor yield fraction is less than 0.1.

Another worry that is not present with this reactor is designing a neutron multiplier. ICF reactors fueled with DT-fueled pellets have a required TBR greater than 1. In order to achieve more than one tritium-producing reaction per source neutron, a neutron multiplier such as beryllium or lead (with favorable $n,2n$ reactions) is required in the blanket to effectively increase the number of neutrons available for reactions in the lithium. However, with the advanced-fuel NPL-driven ICF reactor, the TBR required to sustain operation is much less than 1.0 and can be obtained easily with the small amount of neutron multiplication produced by fissions in the pump gas mixture so that Be- or Pb- containing compounds are not required as neutron multipliers.

Thus, the TBR calculations for the He-cooled NPL-driven ICF reactor blanket indicate that the conceptual design of the reactor and the initial blanket model studied yield a a very reasonable volume for a tritium breeder. The actual breeder need only be a few cubic meters, assuming advanced DD-fueled pellets with ignitor yield fractions near 0.10 can be produced reliably in the future. For this reason, there is a wide choice of possibilities for the exact configuration and location of the breeder in the blanket for self-sustained operation.

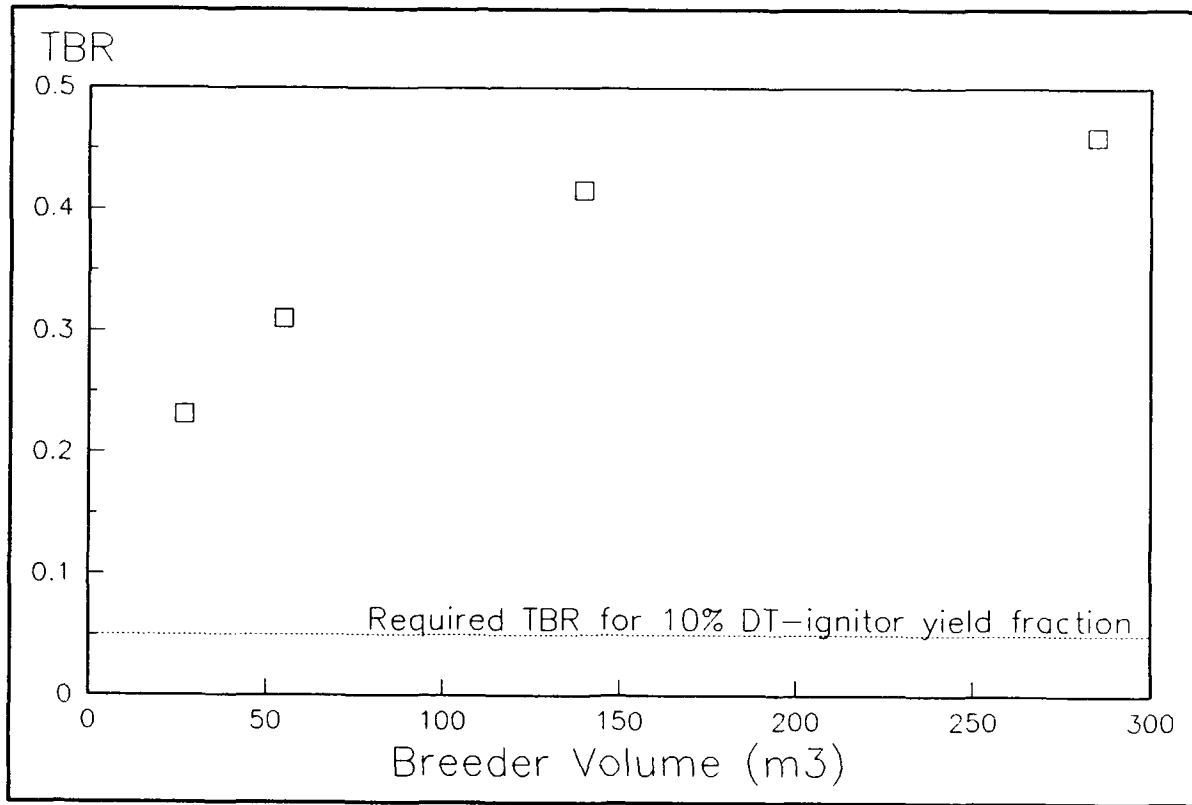


Figure 11. TBR versus the volume of a He-cooled, natural Li_2O breeder.
(Contains HT-9 steel for support and is located just outside blanket fission region.)

IV. Further Work

The initial study of the NPL-driven ICF reactor presented in this paper indicates that the design of an efficient electric plant is feasible in concept. The plant power flow model leads to reasonable ICF pellet injection rates, and the neutronics analysis suggests that the energy multiplication required in the blanket to power an O_2-I_2 nuclear-pumped laser can be obtained with a subcritical fission layer. There are, however, several other design issues which must be addressed in future feasibility studies, some of which are:

1. Design of the magnetic coils which will protect the reactor first wall and divert the charged particles released from the fusion event to collector plates for conversion to electricity. This analysis will involve the solution of the magneto-hydrodynamic equations for a particular set of reactor coils and as accurate a representation of the initial charged-particle spatial and energy distributions as possible.

2. Design of the thermal cycle for removal of heat and conversion to electricity. The study indicated that helium gas and a turbine may be one possible means for heat removal, but that other options such as water, lithium, etc. would also be possible without significantly altering the fission rate and criticality calculations presented in this report for a reactor powered by advanced-fuel ICF pellets.

3. A detailed safety analysis which would address such issues as the build-up of neutron activation products in the blanket and the rate of production of fission products in the nuclear-pumped region of the reactor. A safety analysis would have to consider whether the added complexity caused by the introduction of fission product storage and removal for this type of ICF reactor would be warranted by the possible increase in plant efficiency.

4. A detailed cost analysis for the reactor. An attempt was made in the study to maintain the size of the blanket to what was assumed to be reasonable. However, any eventual decision to design a NPL-driven ICF reactor will be made on the financial merits of constructing such a reactor compared to more conventional fusion design concepts or fission reactors.

V. Summary

This initial study of an O_2-I_2 NPL-driven ICF reactor with magnetically protected walls and advanced-fuel DD pellets indicated that such a concept is feasible. The parametric study of the power flow model and the reactor blanket neutronics calculations yielded no insurmountable obstacles to development of the concept on physical grounds. Rather, improved efficiency over the currently projected DT-fueled ICF reactors is indicated.

The energy and power flow model outlined above suggests that a NPL-driven ICF reactor may operate with advanced-fuel 250-MJ pellets at an injection rate of approximately 6 pellets per second. With a 5 MJ laser driver, the pellet gain of 50 is half that currently projected for DT-fueled ICF reactors, at a reasonable injection rate. The release of 60-75% of advanced-fuel ICF pellet yield as charged particles allows for a high plant net efficiency, approaching or exceeding 50%, because most of the ICF yield can be converted to electricity by a direct conversion process which can be over twice as efficient as a thermal cycle. The plant energy balance demonstrated that the ultimate efficiency obtained will depend on the actual charged-particle yield fraction realized with advanced-fuel pellets and the efficacy with which the reactor magnetic field diverts the ions to collector plates. The 5-MJ NPL requires a blanket energy multiplication of the ICF neutron yield of 2.4 for a reactor 10 m in diameter and 15 m in length. It appears that this required energy multiplication can be feasibly obtained in a reasonably sized blanket. In sum, the conceptual reactor is robust over a wide range of conceivable ICF pellet yields and parameter values.

The neutronics calculations for a cylindrically shaped blanket suggest that the required energy multiplication and the amount of tritium necessary to sustain plant operation can be produced in a reasonably sized blanket. Micropellets consisting of natural uranium oxide or carbide in a nuclear-pumped fissioning layer produced the necessary amount of energy multiplication, assuming the amount of ICF pellet escape neutrons is known. Operating with natural uranium micropellets would help insure the safety of the reactor, found to be very subcritical, if a loss-of-flow accident should occur. Fissions occur at the high-energy end of the spectrum for such micropellets, so that moderation of the fusion neutrons in the blanket first wall and the exact breakout of DT to DDn neutrons is not very significant. However, the energy multiplication calculated is very dependent on the

assumption of the amount of source neutrons (calculated from values taken from the literature). If this value varies significantly, the actual energy multiplication for an NPL-driven ICF reactor operated with DD-fueled pellets will be greatly altered.

The amount of tritium required to maintain continuous plant operation was easily produced with a breeder located just outside the fissioning layer for a variety of advanced DD-fueled pellet make-ups (DT ignitors up to 50% of the pellet yield). In addition, there is no need for a neutron multiplying material like lead or beryllium since the TBR for a DD-fueled pellet is much less than one. The study also indicates there is a large leeway in the size and location of the breeder for this reactor because the required TBR is an order of magnitude smaller than that required for ICF reactors fueled with DT pellets.

The neutronics calculations presented are not found to depend significantly on such factors as the vacuum inside the reactor chamber, the amount of glass inside the nuclear-pumped region, the partial pressures of the oxygen and any buffer gas like argon in the nuclear-pumped region, or the exact design of magnet coils. Thus, there appears to be significant room available for laser and magnet designers to continue developing the conceptual NPL-driven ICF reactor without obviating the neutronics predictions.

Appendix A: Energy Balance TK Solver Model

```

***** VARIABLE SHEET *****
St Input**** Name*** Output*** Unit***** Comment*****
*****Power Cycle Parameters*****
1000  Pnet      nominal power (MWe)
      Wtotal 333.63994 total energy (MJ)
      Ptotal 1946.1789 total power (MW)
      etanet .51382736 net plant efficiency
.15   faux      fraction of Pnet for auxiliary power
      Precirc 150 power recirculated for aux requirement
*****Fusion Reaction Parameters*****
      Q       50 pellet gain
250   Wf        pellet energy yield (MJ)
5     Wd        driver yield on pellet (MJ)
      Pd  29.165857 driver power (MW)
      Wpulse 255 total fusion + driver energy (MJ)
      Rinj  5.8331713 pellet injection frequency (1/s)
*****Partition of Fusion Yield****
.75   fc        plasma fraction of fusion yield
.15   fn        neutron fraction of fusion yield
.1    fx        x-ray fraction of fusion yield
*****Electric Conversion Efficiencies
.85   etadc     direct electric conversion
.4    etath     thermal conversion
.33   etalg     thermal conversion (low-grade) heat
*****Miscellaneous*****
      M       2.377312 required energy multiplication
.33   AR        aspect ratio of blanket (R/L)
      fg      .16539059 geometry factor for cylinder
.01   frad      fraction of Wc to rad from recomb,etc
.9    fb        frac of Wdc diverted to dc converter
.8    etaff     eff for FF escape into pumping medium
.5    etaex     eff for pumping by fission fragments
.5    etacp     eff of chemical/mixing of lasing
.4    etaopt    eff of laser optics
      etal .08 total laser efficiency
*****Fusion Yields & Powers*****
      Pf  1458.2928 fusion pellet power (MW)
      Wx  25 x-ray yield (MJ)
      Px  145.82928 x-ray power (MW)
      Wrad 26.875 radiation energy produced (MJ)
      Wc  187.5 plasma yield (MJ)
      Pc  1093.7196 plasma power (MW)
      Wn  37.5 neutron yield (MJ)
      Pn  218.74393 neutron power (MW)
*****Electric Production (MJ OR MW)***
      Wfwe 15.169026 energy from first wall to electricity
      Pfwe 88.483528 power from first wall to electricity
      Wdce 142.00313 energy from direct conversion
      Pdce 828.32856 power from direct conversion
      Wnthe 39.976181 blanket low-grade energy to electric
      Pnthe 233.18791 blanket low-grade electrical power
      Welec 197.14833 total electric energy per pulse
      Pelec 1150 total average electric power
*****Losses (MJ or MW) *****
      Wfwl 22.753539 first wall energy loss
      Pfwl 132.72529 first wall power loss
      Wdcl 25.059375 energy loss from direct conversion
      Pdcl 146.17563 power loss from direct conversion
      Wnthl 81.163761 low-grade thermal energy loss

```


Pnthl 473.44213 low-grade average thermal power loss
 Wdl 20 driver energy loss
 Pdl 116.66343 driver average power loss
 Wtotlos 136.49161 total energy dumped to environment
 Ptotlos 796.17895 total average power to environment
 *****Others (MJ or MW) *****
 Wdc 167.0625 charged-particle energy available
 Pdc 974.50419 ave. Charged-particle power available
 Wnex 25 energy of excitation of pump medium
 Pnex 145.82928 average excitation power
 Wnth 121.13994 low-grade thermal energy
 Pnth 706.63004 average low-grade thermal power

*****RULE SHEET*****

S Rule *****
 * Q = Wf/Wd
 * Pf = Wf * Rinj
 * fc + fn + fx = 1.00
 * fg = 1 - 1/SQRT(4 * AR^2 + 1) "geometry factor for cylindrical blanket
 * Wpulse = Wd + Wf "Total energy per pellet

"Plasma (Charged-Particle) Energies and Powers

* Wc = fc * Wf
 * Pc = Wc * Rinj
 * Wdc = fb * (1 - frad) * Wc "Total energy collected for direct conversion
 * Pdc = Wdc * Rinj
 * Wdce = Wdc * etadc
 * Pdce = Wdce * Rinj
 * Wdcl = Wdc - Wdce
 * Pdcl = Wdcl * Rinj

"Radiation Energies and Powers

* Wx = fx * Wf
 * Px = Wx * Rinj
 * Wrad = (Wx + frad * Wc) "Radiation from x rays and ions to walls
 * Wfwe = (1 - fg) * etath * (Wrad + (1 - fb) * (1 - frad) * Wc) "first-wall convert
 * Pfwe = Wfwe * Rinj
 * Wfwl = (1 - etath) * (Wfwe/etath)
 * Pfwl = Wfwl * Rinj

"Neutron Energies and Powers

* Wn = fn * Wf
 * Pn = Wn * Rinj
 * Wnex = Wn * (1 - fg) * M * (168/200) * etaff * etaex "population inversion
 * Pnex = Wnex * Rinj
 "small laser low-grade thermal (Wdl) and radiation loss possibly converted
 * Wnth = Wn * (1 + M * (1 - etaex * etaff * (168/200))) + Wdl + fg * Wrad
 * Pnth = Wnth * Rinj
 * Wnthe = Wnth * etalg "low-grade thermal energy to electrical energy
 * Pnthe = Wnthe * Rinj
 * Wnthl = Wnth - Wnthe
 * Pnthl = Wnthl * Rinj

"Laser Energies and Powers

* Wd = Wnex * etacp * etaopt
 * Pd = Wd * Rinj
 * Wdl = Wnex - Wd
 * Pdl = Wdl * Rinj

"Gross/Net Results

* Wtotal = Wc + Wx + Wnth "total available for conversion to electricity
 * Ptotal = Wtotal * Rinj
 * Welec = Wfwe + Wdce + Wnthe "total electrical energy produced
 * Pelec = Welec * Rinj

* $W_{\text{totloss}} = W_{\text{total}} - W_{\text{elec}}$ "total energy loss
 * $P_{\text{totloss}} = W_{\text{totloss}} \cdot R_{\text{inj}}$
 * $P_{\text{net}} = P_{\text{elec}} - P_{\text{circ}}$
 * $\eta_{\text{net}} = P_{\text{net}}/P_{\text{total}}$

"Auxiliary Requirement and Total Laser Efficiency
 * $P_{\text{circ}} = P_{\text{aux}} \cdot P_{\text{net}}$
 * $\eta_{\text{tal}} = \eta_{\text{acp}} \cdot \eta_{\text{opt}} \cdot \eta_{\text{aex}} \cdot \eta_{\text{aff}}$

Appendix B: Sample MORSE Input File

[illegible]

0.0000 +0 0.0000 +0 0.0000 +0 0.0000 +0 0.0000 +0 0.0000 +0
 0.0000 +0 0.0000 +0 0.0000 +0 0.0000 +0 0.0000 +0 0.0000 +0
 0.0000 +0 0.0000 +0 0.0000 +0 0.0000 +0 0.0000 +0 0.0000 +0
 0.0000 +0 0.0000 +0 0.0000 +0 0.0000 +0 0.0000 +0 0.0000 +0
 0.0000 +0 0.0000 +0 0.0000 +0 0.0000 +0 0.0000 +0 0.0000 +0
 0.0000 +0 0.0000 +0 0.0000 +0 0.0000 +0 0.0000 +0 0.0000 +0
 0.0000 +0 0.0000 +0 0.0000 +0 0.0000 +0
 0.0000 +0 0.0000 +0 0.0000 +0 0.0000 +0 0.0000 +0 0.0000 +0
 0.0000 +0 0.0000 +0 0.0000 +0 0.0000 +0 0.0000 +0 0.0000 +0
 0.0000 +0 0.0000 +0 0.0000 +0 0.0000 +0 0.0000 +0 0.0000 +0
 0.0000 +0 0.0000 +0 0.0000 +0 0.0000 +0 0.0000 +0 0.0000 +0
 0.0000 +0 0.0000 +0 0.0000 +0 0.0000 +0 0.0000 +0 0.0000 +0
 0.0000 +0 0.0000 +0 0.0000 +0 0.0000 +0 0.0000 +0 0.0000 +0
 0.0000 +0 0.0000 +0 0.0000 +0 0.0000 +0 0.0000 +0 0.0000 +0
 0.0000 +0 0.0000 +0 0.0000 +0 0.0000 +0

3 0 COMBINATORIAL GEOMETRY NPL-ICF Blanket

RCC	0	0	250.0	0	0	1.5	+3
500.0							
RCC	0	0	250.0	0	0	1.5	+3
510.0							
RCC	0	0	250.0	0	0	1.5	+3
512.0							
RCC	0	0	250.0	0	0	1.5	+3
582.0							
RCC	0	0	250.0	0	0	1.5	+3
607.0							
RCC	0	0	50.0	0	0	1.9	+3
617.0							
RCC	0	0	00.0	0	0	2.0	+3
667.0							
TRC	0	0	1750.0	0	0	2.0	+2
500.0	25.0						
TRC	0	0	250.0	0	0	-2.0	+2
500.0	25.0						
TRC	0	0	1750.0	0	0	2.0	+2
510.0	35.0						
TRC	0	0	250.0	0	0	-2.0	+2
510.0	35.0						
TRC	0	0	1750.0	0	0	2.0	+2
582.0	112.0						
TRC	0	0	250.0	0	0	-2.0	+2
582.0	112.0						
TRC	0	0	1750.0	0	0	2.0	+2
607.0	137.0						
TRC	0	0	250.0	0	0	-2.0	+2
607.0	137.0						
RCC	0	0	-500.0	0	0	3.0	+3
800.0							

END

1	OR	+1OR	+8OR	+9		
2	OR	+2	-1OR	+10	-8OR	+11 -9
3		+3	-2			
4		+4	-3			
5		+13	-11			
6		+12	-10			
7	OR	+5	-4OR	+14	-12OR	+15 -13
8		+6	-5	-14	-15	
9		+7	-6			
10		+16	-7			

END

1	1	1	1	1	1	1	1	1
7	1	2	3	6	6	4	6	5 0

4.0212+9

46 G N CROSS SECTIONS (DABL69) -- P3--

46 46 0 0 69 72 4 7 19 50 4 2 1 3
 0 0 0 0 0 0 0 -10 0 0 0
 SAMBO ANALYSIS INPUT DATA FOR NPL-ICF PROBLEM
 8 45 45 0 0 2 1 1

0.0 0.0 0.0
 0.0 0.0 0.0
 0.0 0.0 0.0
 0.0 0.0 0.0
 0.0 0.0 0.0
 0.0 0.0 0.0
 0.0 0.0 0.0
 0.0 0.0 0.0

RESULTS OF NPL-ICF MORSE CALCULATION (10CM FW, 5CM BRDR, 70CM FIS, 25,30CM R,S)

{fissions/source neutron} fission detector = 1
 0.1979 0.2117 0.2206 0.2247 0.2305 0.2378 0.2466
 0.2563 0.2631 0.2696 0.2773 0.2896 0.3120 0.3265
 0.3350 0.3508 0.3645 0.3702 0.3749 0.3857 0.3860
 0.3975 0.3975 0.3975 0.3975 0.3975 0.4071 0.4071
 0.4071 0.4105 0.4116 0.4125 0.4125 0.4128 0.4129
 0.4131 0.4132 0.4132 0.4132 0.4132 0.4132 0.4132
 0.4132 0.4132 0.4132 0.4132

{T breeding reactions or flux/source neutron} detectors = 2-8
 1.0000 1.0000 1.0000 1.0000 1.0000 1.0000 1.0000
 1.0000 1.0000 1.0000 1.0000 1.0000 1.0000 1.0000
 1.0000 1.0000 1.0000 1.0000 1.0000 1.0000 1.0000
 1.0000 1.0000 1.0000 1.0000 1.0000 1.0000 1.0000
 1.0000 1.0000 1.0000 1.0000 1.0000 1.0000 1.0000
 1.0000 1.0000 1.0000 1.0000 1.0000 1.0000 1.0000
 1.0000 1.0000 1.0000 1.0000

{interactions/energy group}
 2 3 4 5 6 7 8 9 10 11 12 13 14 15
 16 17 18 19 20 21 22 23 24 25 26 27 28 29
 30 31 32 33 34 35 36 37 38 39 40 41 42 43
 44 45 46

\$\$\$\$\$\$\$ NPL-ICF BLANKET JJACOBSON 2 DEC 91 \$\$\$\$\$\$\$

Appendix C: Sample Mixing Input File

```

      0  7 46 46
NPL BLANKET - P3 - NATURAL U (dilute), 1 T BREEDER, HeC FINESSE
46 46 0 0 69 72 4 7 19 39 4 2 1
  0 0 0 0 0 0 0 10 11 0 0
  1 2 3 4 25 26 27 28 31 32 33 34 37 38
39 40 55 56 57 58 61 62 63 64 67 68 69 70
97 98 99 100 121 122 123 124 139 140 141 142 151 152
153 154 157 158 159 160 163 164 165 166 175 176 177 178
181 182 183 184 211 212 213 214 349 350 351 352 385 386
387 388 397 398 399 400
  1 4 1.345E-04 C-12 55 IN FIRST WALL
  1 8 7.200E-05 SI 97
  1 11 1.787E-03 CR 151
  1 12 7.362E-05 MN-55
  1 13 1.234E-02 FE 163
  1 14 6.885E-06 NI 175
  1 -16 8.424E-05 MO 211
  2 2 4.373E-03 LI-6 IN BREEDER
  2 3 5.456E-02 LI-7 IN BREEDER
  2 5 5.984E-05 C-12
  2 7 2.946E-02 O IN LI20
  2 8 3.200E-05 SI
  2 11 7.994E-04 CR
  2 12 3.272E-05 MN
  2 13 5.484E-03 FE
  2 14 3.060E-06 NI
  2 -16 3.744E-05 MO
  3 5 1.000E-05 C-12 IN UC2
  3 7 6.689E-03 O2 AT 76 TORR (0.1 ATM) + GLASS
  3 8 2.000E-03 SI IN GLASS
  3 9 2.687E-05 ARGON AT 760 TORR
  3 18 3.600E-06 U-235 NATURAL
  3 -19 4.640E-04 U-238
  4 5 1.122E-04 C-12 IN PLENUM
  4 8 6.000E-05 SI
  4 11 1.490E-03 CR
  4 12 6.135E-05 MN
  4 13 1.028E-02 FE
  4 14 5.734E-06 NI
  4 -16 7.020E-05 MO
  5 11 1.600E-02 CR IN SHIELD
  5 13 5.745E-02 FE
  5 -14 1.179E-02 NI
  6 6 3.640E-05 N-14
  6 7 4.000E-03 O IN AIR AND GLASS
  6 8 2.000E-03 SI IN GLASS
  6 -15 8.500E-03 CU IN COILS
  7 6 3.640E-07 N IN CAVITY AT .01 ATM
  7 -7 9.740E-08 O2 IN CAVITY AT .01 ATM

```

Appendix D: MORSE FORTRAN Code

```
C      FLUX.FOR
C*****
C*      This version does not determine uncollided fluence.      *
C*      Instead, a tracklength estimator is used to determine   *
C*      fluence and is called for collisions and boundary crossings.*
C*****
C ** THIS IS THE MAIN ROUTINE * * * * *
C ** JJACOBSON 23 OCT 91.
C ** THE FOLLOWING CARD DETERMINES THE SIZE ALLOWED FOR BLANK COMMON *
c ** The value of NLFT below should be set to one less than this size
COMMON NC(1000000)
C ** (REGION SIZE NEEDED IS ABOUT 150K + 4*(SIZE OF BLANK COMMON IN WO
C ** NOTE - THE ORDER OF COMMONS IN THIS ROUTINE IS IMPORTANT AND MUST
C ** POND TO THE ORDER USED IN DUMP ROUTINES SUCH AS HELP, XSCHLP, AN
C **
C ** ASSIGN INPUT AND OUTPUT FILES TO NAM1 AND NAM2 **
CHARACTER*40, NAM1
CHARACTER*40, NAM2
C ** LABELLED COMMONS FOR WALK ROUTINES * * * * *
COMMON /APOLLO/ AGSTRT,DDF,DEADWT(26),ITOUT,ITIN
COMMON /FISBNK/ MFISTP
COMMON /NUTRON/ NAME
C **
C ** LABELLED COMMONS FOR CROSS-SECTION ROUTINES * * * * *
COMMON /LOCSIG/ ISCCOG
COMMON /MEANS/ NM
COMMON /MOMENT/ NMOM
COMMON /QAL/ Q
COMMON /RESULT/ POINT
C **
C ** LABELLED COMMONS FOR GEOMETRY INTERFACE ROUTINES * * * * *
COMMON /GEOMC/ XTWO
COMMON /NORMAL/ UNORM
C **
C ** LABELLED COMMONS FOR USER ROUTINES * * * * *
COMMON /PDET/ ND
COMMON /USER/ AGST
C **
C ** LABELLED COMMON FOR TRITIUM-BREEDING CROSS SECTIONS IN LITHIUM * * * *
REAL SIGT6(46), SIGT7(46), SIGTBR(46), SIGTB6(46), SIGTB7(46)
REAL SG2TB6(46), SG2TB7(46), SG2TBR(46)
COMMON /BREED/ SIGTBR, SIGTB6, SIGTB7, SG2TBR, SG2TB6, SG2TB7
C ** T-BREEDING CROSS SECTIONS FOR LITHIUM-6 AND LITHIUM-7
C ** INITIALIZE SIGT7 (N,N',ALPHA) FOR LITHIUM-7 AND (N,ALPHA) FOR LITHIUM-6
SIGT7(1) = 3.9092E-02
SIGT7(2) = 4.1893E-02
SIGT7(3) = 3.8471E-02
SIGT7(4) = 3.3059E-02
SIGT7(5) = 2.5574E-02
SIGT7(6) = 1.7630E-02
SIGT7(7) = 9.6955E-03
SIGT7(8) = 2.2490E-03
DO 11 I = 9,46
SIGT7(I) = 0
11 CONTINUE
SIGT6(1) = 1.814E-02
SIGT6(2) = 2.256E-02
SIGT6(3) = 2.490E-02
SIGT6(4) = 2.597E-02
```

SIGT6(5) = 2.733E-02
 SIGT6(6) = 2.908E-02
 SIGT6(7) = 3.232E-02
 SIGT6(8) = 4.015E-02
 SIGT6(9) = 4.533E-02
 SIGT6(10) = 5.059E-02
 SIGT6(11) = 5.830E-02
 SIGT6(12) = 7.334E-02
 SIGT6(13) = 8.612E-02
 SIGT6(14) = 9.659E-02
 SIGT6(15) = 1.244E-01
 SIGT6(16) = 1.695E-01
 SIGT6(17) = 2.040E-01
 SIGT6(18) = 2.348E-01
 SIGT6(19) = 2.124E-01
 SIGT6(20) = 1.124E-01
 SIGT6(21) = 1.658E-01
 SIGT6(22) = 0.0730
 SIGT6(23) = 0.0702
 SIGT6(24) = .0393
 SIGT6(25) = .0534
 SIGT6(26) = .0449
 SIGT6(27) = 0.7130
 SIGT6(28) = 0.4551
 SIGT6(29) = 0.3489
 SIGT6(30) = 0.8377
 SIGT6(31) = 0.4963
 SIGT6(32) = 0.5611
 SIGT6(33) = 0.2890
 SIGT6(34) = 1.016
 SIGT6(35) = 1.250
 SIGT6(36) = 1.581
 SIGT6(37) = 3.346
 SIGT6(38) = 5.155
 SIGT6(39) = 6.327
 SIGT6(40) = 3.559
 SIGT6(41) = 2.062E + 1
 SIGT6(42) = 3.599E + 1
 SIGT6(43) = 6.355E + 1
 SIGT6(44) = 1.109E + 2
 SIGT6(45) = 1.829E + 2
 SIGT6(46) = 7.532E + 2

```

C **
TYPE *, '
TYPE *, '***** MORSE Code, NPL-ICF Problem *****'
TYPE *, '= = = = = > WARNING !!! < = = = = = '
TYPE *, 'ABORT if mixed x-secs are not assigned to FOR010'
TYPE *, '
TYPE *, 'ENTER NAME OF INPUT FILE'
ACCEPT 100, NAM1
100  FORMAT(A40)
TYPE *, 'ENTER NAME OF OUTPUT FILE'
ACCEPT 200, NAM2
200  FORMAT(A40)
TYPE *, 'ENTER DENSITY OF LI-6 (ATOMS/BARN-CM) FOR 1ST BREEDER'
READ *, RHO6
TYPE *, 'ENTER DENSITY OF LI-7 (ATOMS/BARN-CM) FOR 1ST BREEDER'
READ *, RHO7
TYPE *, 'ENTER DENSITY OF LI-6 (ATOMS/BARN-CM) FOR 2ND BREEDER'
READ *, RHO26
TYPE *, 'ENTER DENSITY OF LI-7 (ATOMS/BARN-CM) FOR 2ND BREEDER'
READ *, RHO27
  
```



```

C ***** CALCULATE THE MACROSCOPIC T-BREEDING CROSS SECTIONS FOR Li *****
C ***** ARRAYS WITH INDEX 2 REFER TO SECOND TRITIUM BREEDER *****
  DO 12 I = 1,46
    SIGTB6(I) = RHO6 * SIGT6(I)
    SIGTB7(I) = RHO7 * SIGT7(I)
    SIGTBR(I) = SIGTB6(I) + SIGTB7(I)
    SG2TB6(I) = RHO26 * SIGT6(I)
    SG2TB7(I) = RHO27 * SIGT7(I)
    SG2TBR(I) = SG2TB6(I) + SG2TB7(I)
12  CONTINUE
  OPEN(UNIT=1,NAME=NAM1,TYPE='OLD')
  OPEN(UNIT=2,NAME=NAM2,TYPE='NEW')
  ITOUT = 2
  ITIN = 1
  NLFT = 999999
  CALL MORSE(NLFT)
  TYPE 300, NAM2
300  FORMAT(X,'OUTPUT FILE IS ',A40)
  STOP
  END

  SUBROUTINE GTMED(MDGEOM,MDXSEC)
C  THIS VERSION EQUATES X-SECTION WITH GEOMETRY MEDIA
  MDXSEC = MDGEOM
  RETURN
  END

  FUNCTION DIREC(F)
  direc = 1
  RETURN
  END

  SUBROUTINE BANKR(NBNKID)
C  DO NOT CALL EUCLID FROM BANKR(7)
  COMMON /APOLLO/ AGSTRT,DDF,DEADWT(5),ETA,ETATH,ETAUSD,UNP,VINP,
  1 WINP,WTSTRT,XSTRT,YSTRT,ZSTRT,TCUT,XTRA(10),
  2 I0,I1,MEDIA,IADJM,ISBIAS,ISOUR,ITERS,ITIME,ITSTR,LOCWTS,LOCFWL,
  3 LOCEPR,LOCNSC,LOCFSN,MAXGP,MAXTIM,MEDALB,MGPREG,MXREG,NALB,
  4 NDEAD(5),NEWNM,NGEOM,NGPQT1,NGPQT2,NGPQT3,NGPQTG,NGPQTN,NITS,
  5 NKCALC,NKILL,NLAST,NMEM,NMGP,NMOST,NMTG,NOLEAK,NORMF,NPAST,
  6 NPSCL(13),NQUTT,NSIGL,NSOUR,NSPLT,NSTRT,NXTRA(10)
  COMMON /NUTRON/ NAME,NAMEX,IG,IGO,NMED,MEDOLD,NREG,U,V,W,UOLD,VOLD
  1 ,WOLD,X,Y,Z,XOLD,YOLD,ZOLD,WATE,OLDWT,WTBC,BLZNT,BLZON,AGE,OLDAGE
  NBNK = NBNKID
  IF (NBNK) 100,100,140
  100 NBNK = NBNK + 5
  GO TO (104,103,102,101),NBNK
  101 CALL STRUN
C  CALL HELP(4HSTRU,1,1,1,1)
  RETURN
  102 NBAT = NITS - ITERS
  NSAVE = NMEM
  CALL STBTCH(NBAT)
C  NBAT IS THE BATCH NO. LESS ONE
  RETURN
  103 CALL NBATCH(NSAVE)
C  NSAVE IS THE NO. OF PARTICLES STARTED IN THE LAST BATCH
  RETURN
  104 CALL NRUN(NITS,NQUTT)
C  NITS IS THE NO. OF BATCHES COMPLETED IN THE RUN JUST COMPLETED
C  NQUTT .GT. 1 IF MORE RUNS REMAIN
C  .EQ. 1 IF THE LAST SCHEDULED RUN HAS BEEN COMPLETED
C  IS THE NEGATIVE OF THE NO. OF COMPLETE RUNS, WHEN AN
C  EXECUTION TIME KILL OCCURS

```

```

      RETURN
140 GO TO (1,2,3,4,5,6,7,8,9,10,11,12,13),NBNK
C NBNKID COLL TYPE BANKR CALL NBNKID COLL TYPE BANKR CALL
C 1 SOURCE YES (MSOUR) 2 SPLIT NO (TESTW)
C 3 FISSION YES (FPROB) 4 GAMGEN YES (GSTORE)
C 5 REAL COLL YES (MORSE) 6 ALBEDO YES (MORSE)
C 7 BDRYX YES (NXTCOL) 8 ESCAPE YES (NXTCOL)
C 9 E-CUT NO (MORSE) 10 TIME KILL NO (MORSE)
C 11 R R KILL NO (TESTW) 12 R R SURV NO (TESTW)
C 13 GAMLOST NO (GSTORE)
1 RETURN
2 RETURN
3 RETURN
4 RETURN
5 CALL TRKCOL
  RETURN
6 RETURN
7 CALL TRKBDR
  RETURN
8 RETURN
9 RETURN
10 RETURN
11 RETURN
12 RETURN
13 RETURN
  END
      SUBROUTINE TRKBDR
C*****
C this version determines flux as tracklength divided by detector
C volume.
C MEDIA: 1 - FIRST WALL/OUTER REFLECTOR = GRAPHITE
C 2 - FIRST WALL COOLANT/T BREEDER
C 3 - FISSION BLANKET
C 4 - OUTER PLENUM
C*****
COMMON /PDET/ ND,NNE,NE,NT,NA,NRESP,NEX,NEXND,NEND,NDNR,NTNR,NTNE,
1 NAME,NTNDNR,NTNEND,NANEND,LOCSP,LOCXD,LOCIB,LOCCO,LOCT,LOCUD,
2 LOCSD,LOCQE,LOCQT,LOCQTE,LOCQAE,LMAX,EFIRST,EGTOP
COMMON /NUTRON/ NAME,NAMEX,IG,IGO,NMED,MEDOLD,NREG,U,V,W,UOLD,VOLD
1 ,WOLD,X,Y,Z,XOLD,YOLD,ZOLD,WATE,OLDWT,WTBC,BLZNT,BLZON,AGE,OLDAGE
COMMON /BREED/ SIGTBR(46),SIGTB6(46),SIGTB7(46),SG2TBR(46),
1 SG2TB6(46),SG2TB7(46)
      C *** check for neutron not coming from fission blanket ***
      R = SQRT(X**2 + Y**2)
      IF (R.LE.510.OR.R.GT.582.OR.Z.LT.250.OR.Z.GT.1750) RETURN
      C *** add track length to zone detector ***
      TRK = WATE * SQRT((X-XOLD)**2 + (Y-YOLD)**2 + (Z-ZOLD)**2)
      C *** flux = trk/vol
      c *** nusigf/nu * flux * vol is fission reaction rate
c * division by nu is done in detector response function in npl.in

      IF (R.GT.515.AND.R.LE.582) THEN
      NDETEC = 1
      CALL FISGEN(IG,MEDOLD,PNUF)
      CALL NSIGTA(IG,MEDOLD,SIGT,PNAB)
      CON = TRK * SIGT * PNUF
      CALL FLUXST(NDETEC,IG,CON,0.0,0.0,0)
      NDETEC = 2
      VOL = 3.6E+8
      CON = TRK / VOL
      CALL FLUXST(NDETEC,IG,CON,0.0,0.0,0)
      GO TO 102
      END IF

```

```

      C *** TRITIUM-PRODUCTION RATE = TRK * SIGTBR
C *** FOR CURRENT ENERGY GROUP
C *** DETECTORS 3-5 ARE FOR 1ST T BREEDER ***
C *** DETECTORS 6-8 ARE FOR 2ND T BREEDER ***
      IF (R.GT.510.AND.R.LE.512) THEN
        CON = TRK * SIGTB6(IG)
        NDETEC = 3
        CALL FLUXST(NDETEC,IG,CON,0.0,0.0,0)
        CON = TRK * SIGTB7(IG)
        NDETEC = 4
        CALL FLUXST(NDETEC,IG,CON,0.0,0.0,0)
        CON = TRK * SIGTBR(IG)
        NDETEC = 5
        CALL FLUXST(NDETEC,IG,CON,0.0,0.0,0)
      ELSE
        CON = TRK * SG2TB6(IG)
        NDETEC = 6
        CALL FLUXST(NDETEC,IG,CON,0.0,0.0,0)
        CON = TRK * SG2TB7(IG)
        NDETEC = 7
        CALL FLUXST(NDETEC,IG,CON,0.0,0.0,0)
        CON = TRK * SG2TBR(IG)
        NDETEC = 8
        CALL FLUXST(NDETEC,IG,CON,0.0,0.0,0)
      END IF
      C *SWITCH = 0 -- STORE IN ALL RELEVANT ARRAYS EXCEPT UD
102 RETURN
END

      SUBROUTINE TRKCOL
C*****
C this version determines flux from tracklength divided by detector
C volume and is used with TRKBDR (called from BANKR(7))
C*****
COMMON /PDET/ ND,NNE,NE,NT,NA,NRESP,NEX,NEXND,NEND,NDNR,NTNR,NTNE,
1 NANE,NTNDNR,NTNEND,NANEND,LOCRSP,LOCXD,LOCIB,LOCCO,LOCT,LOCUD,
2 LOCSD,LOCQE,LOCQT,LOCQTE,LOCQAE,LMAX,EFIRST,EGTOP
COMMON /NUTRON/ NAME,NAMEX,IG,IGO,NMED,MEDOLD,NREG,U,V,W,UOLD,VOLD
1 ,WOLD,X,Y,Z,XOLD,YOLD,ZOLD,WATE,OLDWT,WTBC,BLZNT,BLZON,AGE,OLDAGE
COMMON /BREED/ SIGTBR(46),SIGTB6(46),SIGTB7(46),SG2TBR(46),
1 SG2TB6(46),SG2TB7(46)
      C *** check for fission blanket or tritium breeder ***
      R = SQRT(X**2 + Y**2)
      IF (R.LE.510.OR.R.GT.582.OR.Z.GT.1750.OR.Z.LT.250) RETURN
      C *** calculate fluence estimate
      TRK = WTBC * SQRT((X-XOLD)**2 + (Y-YOLD)**2 + (Z-ZOLD)**2)
C *** # of abs. neutrons = flux * vol * siga
C *** but flux = trk/vol
      c *** nusigf/nu * flux * vol is fission reaction rate
c * division by nu is done in detector response function in npl.in

      IF (R.GT.515.AND.R.LE.582) THEN
        NDETEC = 1
        CALL FISGEN(IGO,MEDOLD,PNUF)
        CALL NSIGTA(IGO,MEDOLD,SIGT,PNAB)
        CON = TRK * SIGT * PNUF
        CALL FLUXST(NDETEC,IGO,CON,0.0,0.0,0)
        NDETEC = 2
        VOL = 3.6E+8
        CON = TRK / VOL
        CALL FLUXST(NDETEC,IGO,CON,0.0,0.0,0)
        GO TO 102
      END IF

```

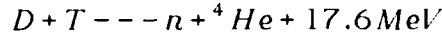
```

      C *** T-BREEDING RATE = TRK * SIGTBR FOR OLD ENERGY GROUP
C *** DETECTORS 3-5 ARE FOR 1ST T BREEDER ***
C *** DETECTORS 6-8 ARE FOR 2ND T BREEDER ***
      IF (R.GT.510.AND.R.LE.512) THEN
        CON = TRK * SIGTB6(IGO)
        NDETEC = 3
        CALL FLUXST(NDETEC,IGO,CON,0.0,0.0,0)
        CON = TRK * SIGTB7(IGO)
        NDETEC = 4
        CALL FLUXST(NDETEC,IGO,CON,0.0,0.0,0)
        CON = TRK * SIGTBR(IGO)
        NDETEC = 5
        CALL FLUXST(NDETEC,IGO,CON,0.0,0.0,0)
      ELSE
        CON = TRK * SG2TB6(IGO)
        NDETEC = 6
        CALL FLUXST(NDETEC,IGO,CON,0.0,0.0,0)
        CON = TRK * SG2TB7(IGO)
        NDETEC = 7
        CALL FLUXST(NDETEC,IGO,CON,0.0,0.0,0)
        CON = TRK * SG2TBR(IGO)
        NDETEC = 8
        CALL FLUXST(NDETEC,IGO,CON,0.0,0.0,0)
      END IF
      102 RETURN
END

```

Appendix E

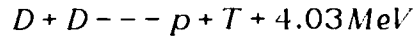
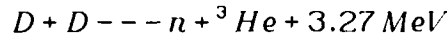
The TBR required to sustain plant operations is calculated in the following manner. The number of tritons required per pellet to sustain plant operation is calculated by considering the reaction



which indicates that 17.6 MeV is released by each DT reaction in the ignitor. The number of DT reactions which occur in the ignitor, hence the number of tritons which must be replaced is then

$$N_T = \frac{f_{ig} W_f}{(17.1 \text{ MeV})(1.602 \times 10^{-19} \text{ MJ/MeV})}$$

where N_T is the number of T reactions required and W_f is the fusion yield of the pellet. It is also the theoretical number of 14.1-MeV neutrons released by the ignitor. In the fuel, two reactions are assumed to take place equally frequently since their cross sections at temperatures of interest (10-100 keV) do not differ significantly:



Because the likelihood of a DT reaction occurring is about an order of magnitude greater than the two reactions above, the DT reaction is assumed to be partially catalyzed by the DDp reaction, so that the three reactions can be considered to yield one overall reaction in the fuel in which 5 deuterons combine to produce 2 neutrons, 1 proton, 1 ${}^3\text{He}$ nucleus, and an alpha particle with 24.89 MeV of energy released. The number of these reactions in the fuel is then simply

$$N_{5D} = \frac{(1 - f_{ig}) W_f (\text{MJ})}{(24.89 \text{ MeV})(1.602 \times 10^{-19} \text{ MJ/MeV})}$$

where N_{5D} is the total number of reactions in the fuel. The required TBR is then defined as the number of tritium required per source neutron or

$$\text{Required TBR} = \frac{N_T}{(N_T + 2N_{5D})}$$

In a similar manner, the average source neutron energy can be calculated. The following TK-Solver routine was used to perform a parameter study of the required TBR and average neutron energy as a function of the DT-ignitor yield fraction.

```

***** VARIABLE SHEET *****
St Input**** Name*** Output*** Unit***** Comment*****
      Wig  2.5          Ignitor Yield (MJ)
L 'Fdt    Fdt          Fraction of fusion yield in ignitor
  250     Wf           Fusion Yield (MJ)
      Numdt 8.8668E17   Number of ignitor DT reactions
      Wfuel 247.5       Fusion Yield (MJ) in pellet DD fuel
      Numfuel 6.2046E19 Number of DDn + DDp + DT reactions in fuel
      Totaln 1.2498E20 Total number of neutrons produced
L      Tpern .00709462  Required tritium per source neutron
L      Enave 8.3570701  Average neutron energy (MeV)

```

```

***** RULE SHEET *****
S Rule*****
* Wig = Fdt * Wf
* Numdt = Wig/(17.6 * 1.602e-19)
* Wfuel = (1-Fdt) * Wf
* Numfuel = Wfuel/(24.9 * 1.602e-19)
* Totaln = Numdt + 2 * Numfuel
* Tpern = Numdt / Totaln
* Enave = (Numdt*14.1 + Numfuel*8.275) / (Numdt + Numfuel)

```

Bibliography

1. Lawrence Livermore National Laboratory. Inertial Confinement Fusion. Laboratory Brochure CRO 89/146 10M 7/AP 89/JR, April 1989.
2. Miley, George H. Fusion Energy Conversion. United States: American Nuclear Society, 1976.
3. Basov, Y. G. "Nontraditional Method of Laser Pumping," Pribory i Tekhnika Eksperimenta, 6: 5-17 (1988).
4. Chung, A. K. and Prelas M. A. "Charged particle spectra from U-235 and B-10 micropellets and slab coatings," Laser and Particle Beams, 2: 201-211 (1984).
5. Miley, George H. "Neutron feedback inertial confinement fusion," Atomkernenergie-Kerntechnik, 45: 14-18 (1984).
6. Shiba, T. and others. "Burn Characteristics of D-T ignited D-D and D-³He Fuel Pellets for Inertial Confinement Fusion Reactors," Nuclear Fusion, 28: 699-705 (1988).
7. Beller, D. E. and others. "Parametric Design Space and Nuclear Analysis of a Nuclear-Pumped-Laser-Driven ICF Reactor," Fusion Technology, 15: 772-777 (March 1989).
8. Ingersol, D. T. and others. DABL69: A Broad-Group Neutron/Photon Cross-Section Library for Defense Nuclear Applications. Report ORNL/TM-10568. Oak Ridge National Laboratory, June 1989.
9. Oak Ridge National Laboratory. MORSE-CG: General Purpose Monte Carlo Multigroup Neutron and Gamma-Ray Transport Code with Combinatorial Geometry. ORNL-4972/R2. Oak Ridge National Laboratory, July 1984.
10. Monsler, M. J. and others. "An Overview of Inertial Fusion Reactor Design," Nuclear Technology/Fusion, 1: 302-358 (July 1981).
11. Dolan, T. J. Fusion Research: Volume 1 - Principles. New York: Pergamon Press, 1982.
12. Bohachevsky, I. O. and others. "Plasma Behavior in Magnetically Protected Inertial Confinement Fusion Reactor Cavities," Nuclear Technology/Fusion, 1: 390-401 (July 1981).
13. FINESSE Phase I Report. Technical Issues and Requirements of Experiments and Facilities for Fusion Nuclear Technology, Vol I and II. UCLA-ENG-85-39. University of California, Los Angeles, 1985.

Vita

Captain John M. Jacobson was born on 18 April 1962 in Syracuse, New York. He graduated from the Christian Brothers Academy in Syracuse in 1980 and attended the College of the Holy Cross in Worcester, Massachusetts. He graduated with a Bachelor of Science in Physics in May of 1984. After graduation, he entered active duty at Wright-Patterson AFB where he served for six years as a missile systems analyst for the Foreign Technology Division until he was selected to attend the Air Force Institute of Technology. He married his beautiful wife, the former Jennifer M. Glidewell, in March of 1990, and currently resides with her and two wonderful step-children: Amanda and Zachary.

Home of Record:

RD #2 Box 771

West Monroe, NY, 13167